CYTOTOXICITY AND ANTIOXIDANT ACTIVITY OF SYNTHESIZED SILVER NANOPARTICLES FROM *Artemisiae scopariae* LEAF EXTRACT

BY

TAY SOON GHEE

A project report submitted to the Department of Biomedical Science

Faculty of Science

Universiti Tunku Abdul Rahman

In partial fulfilment of the requirements for the degree of

Bachelor of Science (Hons)

Biomedical Science

April 2019

ABSTRACT

CYTOTOXICITY AND ANTIOXIDANT ACTIVITY OF SYNTHESIZED SILVER NANOPARTICLES FROM *Artemisiae scopariae* LEAF EXTRACT

Tay Soon Ghee

Nanomedicine relates to the utilization of precisely engineered nanomaterial to aid in the diagnostic and therapeutic procedures for human uses. Synthesis of silver nanoparticles using plant extracts is a very cost-effective, simple and environmentally friendly method. The current study demonstrates the green synthesis of silver nanoparticles from leaf extract of *Artemisiae scopariae*. *Artemisiae scopriae* is a Chinese herb from the family Asteraceae with beneficial medicinal properties such as antipyretic, antioxidant and anticancer. The objective of the study was to evaluate the effectiveness of the synthesized silver nanoparticles using *Artemisiae scopariae* for cytotoxic and antioxidant activities. Aqueous extract of *Artemisiae scopariae* was obtained by boiling the herb with distilled water for 30 minutes and further freeze dried for lyophilization. Silver nanoparticles were synthesized using aqueous extract of *Artemisiae scopariae* and silver salt. Color changes from dark brown to reddish brown after 24 hours synthesis indicates the reduction of Ag^+ ion to Ag atom. The synthesized silver nanoparticles were further characterized using ultraviolet-visible spectroscopy (UV-Vis). The absorption peaks in the range of 325 to 455 nm were observed due to the excitation of surface plasmon resonance in the presence of secondary

metabolites. The synthesized silver nanoparticles were evaluated for antioxidant activity through 2,2-diphenyl-1-picrylhydrazyl (DPPH) assay. In DPPH assay, silver nanoparticles (AgNPs) at ratio 9:1 exhibited strong radical scavenging activity with EC_{50} of 0.013 mg/mL. The cytotoxicity of silver nanoparticles was determined via thiazolyl blue tetrazolium bromide (MTT) assay. In MTT assay, AgNPs at ratio 1:9 exhibited cytotoxicity against HeLa cells with the IC_{50} of 2.144 µg/mL after 24 hours, while AgNPs at ratio 1:1 showed IC_{50} of 2.747 µg/mL against HT-29 cells after 48 hours treatment. Hence, the preliminary screening of the green synthesized silver nanoparticles exhibited potent cytotoxicity and antioxidant activity. Thus, the silver nanoparticles can be further analyzed for other biological activities to ease in cancer drug discovery.

ACKNOWLEDGEMENTS

I would like to express my sincere gratitude to my supervisor, Miss Sangeetha a/p Arullappan for providing guidance and support to me throughout this research project.

Furthermore, I would like to express my appreciation to the university UTAR for giving me an opportunity to complete my final year project with the facilities and equipment. I would also like to thank laboratory officers and postgraduates in UTAR for helping me in the operation and utilization of the equipment and also share with me their experience in this research.

Last but not least, I would like to express my gratitude to my family and friends for their moral support throughout this research project.

DECLARATION

I hereby declare that this final year project report is based on my original work except for quotations and citations which have been duly acknowledged. I also declare that it has not been previously or concurrently submitted for any other degree at UTAR or other institutions.

_____

Tay Soon Ghee

APPROVAL SHEET

This final year project report entitled "**CYTOTOXICITY AND ANTIOXIDANT ACTIVITY OF SYNTHESIZED SILVER NANOPARTICLES FROM *Artemisiae scopariae* LEAF EXTRACT**" was prepared by TAY SOON GHEE and submitted as partial fulfilment of the requirements for the degree of Bachelor of Science (Hons) Biomedical Science at Universiti Tunku Abdul Rahman.

Approved by:

_____

(Ms. Sangeetha A/P Arullappan) Date:……..

Supervisor

Department of Biomedical Science

Faculty of Science

Universiti Tunku Abdul Rahman

FACULTY OF SCIENCE

UNIVERSITI TUNKU ABDUL RAHMAN

Date: _____

PERMISSION SHEET

It is hereby certified that TAY SOON GHEE (ID No: 15ADB03101) has completed this final year project thesis entitled "**CYTOTOXICITY AND ANTIOXIDANT ACTIVITY OF SYNTHESIZED SILVER NANOPARTICLES FROM *Artemisiae scopariae* LEAF EXTRACT**" under the supervision of Ms. Sangeetha A/P Arullappan (Supervisor) from the Department of Biomedical Science, Faculty of Science.

I hereby give permission to the University to upload the softcopy of my final year project thesis in pdf format into the UTAR-Institutional Repository, which may be made accessible to the UTAR community and public.

Yours truly,

_____

(TAY SOON GHEE)

TABLE OF CONTENTS

LIST OF TABLES

LIST OF FIGURES

LIST OF ABBREVIATIONS

ABTS	2,2'-azino-bis(3-ethylbenzothiazoline-6-sulphonic acid)
Ag^+	Silver ion
$AgNO_3$	Silver nitrate
AgNPs	Silver nanoparticles
ATCC	American Type Culture Collection
ATP	Adenosine triphosphate
DMEM	Dulbecco's Modified Eagle Medium
DMSO	Dimethyl sulfoxide
DNA	Deoxyribonucleic acid
DPPH	α, α-diphenyl-βpicrylhydrazyl
EC_{50}	Half-maximal effective concentration
FRAP	Ferric reducing antioxidant power
FTIR	Fourier transform infrared spectroscopy
IC_{50}	Half-maximal inhibitory concentration
MTT	3-(4,5-dimethylthiazol-2-yl)-2,5-diphenyltetrazolium bromide
NCI	National Cancer Institute
PBS	Phosphate buffered saline
ROS	Reactive oxygen species
SPR	Surface plasmon resonance
TEM	Transmission electron microscopy
UV-Vis	Ultraviolet-Visible

CHAPTER 1

INTRODUCTION

1.1 Silver Nanoparticles

Nanotechnology is a term derived from Greek word which means dwarf that applies to engineering, electronics and material sciences in molecular or submicron level. A prominent promoter of nanotechnology, Albert Franks, define nanotechnology as “the field of science and technology where the dimensions and tolerances are within the range of 0.1 to 100 nm” (Sahoo and Labhasetwar, 2003). Within this size, all the chemical, physical and biological properties varies fundamentally in terms of individual atoms or molecules with their corresponding bulk. Novel applications of nanotechnology is growing exponentially due to their entirely new or improved properties based on size, distribution and morphology. Nanotechnology has been used widely in biomedical applications, such are gene therapy, drug delivery and imaging (Sahoo and Labhasetwar, 2003; Ahmed et al., 2016).

One of the essential branches in nanotechnology is the development of green synthesis of nanoparticles (Safaepour et al., 2009). Green synthesis of nanoparticles refers to a process that reduces or eliminates the usage of toxic substances for human health and environment by introducing new chemical ways without pollution (Heydari and Rashidipour, 2015). Conventionally,

nanoparticles are synthesized using physical and chemical methods. Biological approaches of synthesizing silver nanoparticles is the green chemical reaction that utilizes plants, plant products, bacteria, fungi, algae, yeast and viruses. Biological method is not only environmental friendly, but also provides a better control over the shape, size and morphology. Biological approaches gain its merits from conferring physiological solubility and stability to the nanoparticles, which is the criteria for biomedical applications. The advantages of biological method in the synthesis of nanoparticles are lower toxicity, cost efficient, biocompatibility and prominent dispersity (Gurunathan et al., 2013).

Metallic nanoparticles exert significant antibacterial properties due to their high surface area to volume ratios. Comparing to all the noble metal nanoparticles, silver nanoparticles are an arch product in nanotechnology due to their good conductivity, catalytic, antifungal, antibacterial and antiviral activities. Silver nanoparticles have been applied in composite fibers, cryogenic superconducting fibers, wound dressings and food industry. Silver nanoparticles lately being applied in cancer diagnosis and treatment (Ahmed et al., 2016). However, prolonged exposure to higher doses of silver nanoparticles will cause toxicity such as argyria (Lansdown, 2010).

Green synthesis of silver nanoparticles involves the mixing of natural product such as plant extracts with metal salts. Plant extracts serve as reducing and stabilizing agents for the synthesis. Plant extracts will reduce silver salt solution to form silver nanoparticles. Two processes are recognized in the formation of silver nanoparticles. The first phase is the nucleation phase in which the silver

atoms use high activation energy to form small nucleases. The second phase is known as growth phase, whereby these small nucleases combine together and form the silver nanoparticles. Since silver possesses high reduction potential, once the formation of silver nanoparticles completed, the particles can be collected aqueous solution free of stabilizer (Carmona et al., 2017).

1.2 Cancer

Cancer is the second leading cause of death worldwide and accounted for 8.8 million deaths in 2015. Globally, almost 1 in 6 deaths is caused by cancer (World Health Organization, 2018). Cancer refers to a collection of diseases characterized by the abnormal growth of cells with the ability to invade and metastasize. Cancer can begin in anywhere in the human body. Under normal circumstances, normal cells grow and divide to replace the old or damaged cells. However, cancer cells do not follow these signals. Cancer cells do not undergo apoptosis when there is damaged to the cell, but it continues to proliferate continuously. Cancer is a genetic disease cause by mutation into respective genes that control the cells function, particularly on how the cells grow and divide. The environmental factors that also can cause cancer are chemicals in tobacco smoke and radiation such as ultraviolet ray emitted from the sun (National Cancer Institute, 2015).

1.3 Problem Statement

To date, there is only a few studies on the green synthesis of silver nanoparticles using *Artemisiaee scopariae* and their evaluation of biological activities. Many cancers respond to chemotherapy in the beginning, but in the later stage cancers develop resistance against the chemotherapy. These chemopreventives and chemotherapeutic agents will lead to undesirable side effects. Producing a biocompatible and cost-effective approach to treat cancers is very important. Cytotoxic agents used in chemotherapy are of high cost and known to cause several side effects, such as anemia and most crucially the generation of cellular resistance. Thus, it is a paramount to search for alternative therapies or medicines to solve this crisis (Gurunathan et al., 2013).

Research into green synthesis of silver nanoparticles is part of an attempt to reduce cancer cases and other diseases. The present study focused on the cytotoxicity and antioxidant activity of silver nanoparticles synthesized from *A. scopariae* leaf extract. The synthesized silver nanoparticles were evaluated for cytotoxicity and antioxidant activity.

1.4 Objectives

1. To synthesize silver nanoparticles using aqueous extract of *Artemisiae scopariae* and silver salt,
2. To characterize the presence of synthesized silver nanoparticles using UV-vis spectrophotometer,
3. To determine the percentage of cell viability of cancer cell lines treated with silver nanoparticles using MTT assay,
4. To evaluate the radical scavenging activity of the synthesized silver nanoparticles using DPPH assay.

CHAPTER 2

LITERATURE REVIEW

2.1 *Artemisiae scopariae*

2.1.1 Botanical Description

The Chinese name of *Artemisiae scopariae* as shown in **Figure 2.1** is 茵陳 (Yinchen) (Singh and Sarin, 2010). The herb is usually collected during spring when the seedling is 6 to 10 cm high, or in autumn when the bud is forming. The herb collected in spring is referred as "Mianyinchen" and while in autumn is referred as "Yinchenhao". *Artemisiae scopariae* is originated from China particularly the Shaanxi, Shanxi and Anhui provinces, Japan and Taiwan. The stems of Yinchenhao is cylindrical, pubescent with light texture, fragile, fracture, white and branched with the length of 30 to 100 cm long and is 2 to 8 mm in diameter. The exterior of the herb is purple in color and striated longitudinally. The leaves are crowded, or most of it fallen off (Wagner et al., 2011). The basal leaves are two to three pinnatipartite, stripe in shape and crowded with white color pubescences, cauline leaves with one to two pinnatipartisect, amplexicaul, filamentous and the capitulum is ovoid. The leaves are usually 1.2 to 1.5 mm long with the diameter of 1.0 to 1.2 mm. The odor is aromatic while the taste is bitter (Wagner et al., 2011).

Figure 2.1: Fresh *A. scopariae* (Adapted from Singh and Sarin, 2010).

The collection of the herbs in different seasons affect its therapeutic effects significantly. According to traditional Chinese medicine, *A. scopariae* has to be harvested in April because the herbs collected in May is believed to have no medicinal values. However, modern chemical and pharmacological investigations shown that *A. scopariae* should be harvested in August or September (Tan et al., 2008).

2.1.2 Geographical Distribution

A. scopariae is distributed around the sandy places along the sea coast in South Korea and India (Cha et al., 2005; Singh et al., 2009). The herb is categorized as an aromatic herbaceous annual plant and also can be found in the wastelands of the north part of India. It is distributed from Central Europe to Western Asia,

which includes China, Japan, India, and Afghanistan and extends up to 2.1 km in the western Himalayas (Singh et al., 2009).

2.1.3 Taxonomical Classification

The taxonomical classification of *Artemisiae scopariae* is shown in **Table 2.1**. The plant generally known as Redstem wormwood from the family of Asteraceae.

Table 2.1: Taxonomical classification of *Artemisiae scopariae* (Database of Medicinal and Aromatic Plants in Rajasthan, 2016).

Rank	**Taxonomical Classification**
Kingdom	Plantae
Subkingdom	Tracheobionta
Division	Magnoliophyta
Class	Magnoliopsida
Subclass	Asteridae
Order	Asterales
Family	Asteraceae
Genus	*Artemisiae*
Species	*scopariae*

2.1.4 Chemical Constituents

The chemical constituents of *A. scopariae* were analyzed using high performance liquid chromatography and diode array detection. A total of 13 bioactive compounds were detected in *A. scopariae*, namely chlorogenic acid, 6, 7–dihydroxycoumarin, caffeic acid, 4-hydroxyacetophenone, scopoletin, rutin, hyperoside, isoquercitrin, 3, 5-dicaffeoylquinic acid, 4, 5-dicaffeoylquinic acid, scoparone, 7-methoxycoumarine and quercetin are shown in **Figure 2.2** (Tan et al., 2008). The concentration of the constituents are dependent on collection of every seasons. The herbs have the highest concentration of chlorogenic acid in spring. The concentration of caffeic acid, 3, 5-dicaffeoylquinic acid, 4, 5-dicaffeoylquinic acid and 4-hydroxyacetophenone increases from May to July. The phenolic acids, coumarins, flavonoids and 4-hydroxyacetophenone in *A. scopariae* have the potential to serve as the "marker compounds" for the chemical evaluation and standardization of *A. scopariae* (Tan et al., 2008).

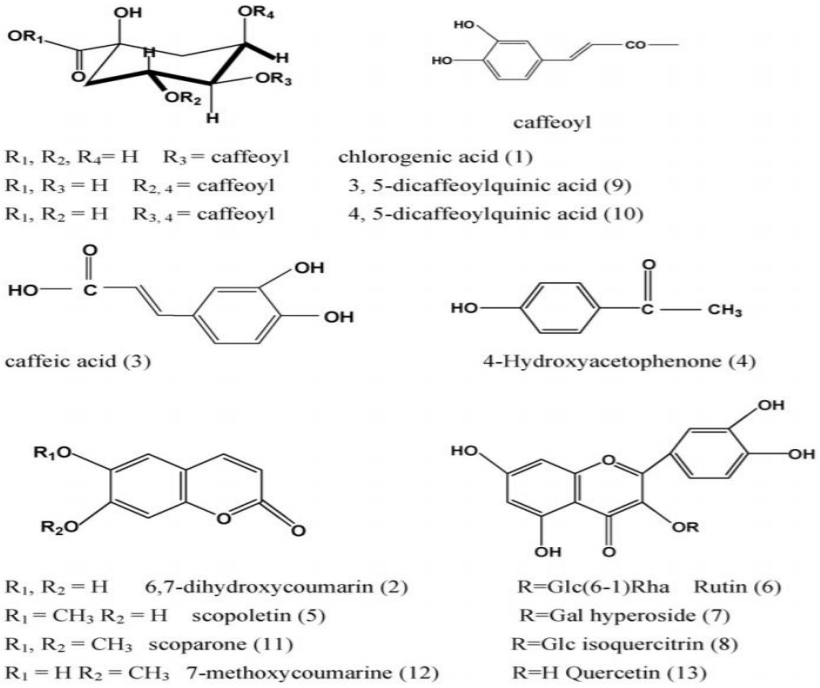

Figure 2.2: The chemical structures found in *A. scopariae* .Chlorogenic acid (1), 6,7-dihydroxycoumarin (2), caffeci acid (3), 4-hydroxyacetophenone (4), scopaletin (5), rutin(6), hyperoside (7), isoquercitrin (8), 3,5-dicaffeoylquinic acid (9), 4, 5-dicaffeiylquinic acid (10), scoparone (11), 7-mthoxycoumarine (12) and quercetin (13)(Adapted from Tan et al., 2008).

2.2 Previous Investigation of *A. scopariae*

2.2.1 Anti-inflammatory Activity

Habib and Waheed (2013) reported that the *A. scopariae* hydromethanolic extract with the concentration of 400 mg/kg and 500 mg/kg exhibited a significant anti-inflammatory effect in the late phase about 3 to 4 hours of carrageenan induced paw edema. The reduction of carrageenan induced paw edema in rats was up to 74%. The early phase approximately 2.5 hours of this method involve in the release of inflammatory mediators such as serotonin and bradykinins, whereas the late phase of carrageenan induced paw edema is linked with the release of prostaglandin. The inhibitory effect in the late phase indicated

the possible inhibitory effect towards the release prostaglandins so the extract can be used to treat local inflammation.

2.2.2 Antinociceptive Activity

Hydromethanolic extract of *A. scopariae* significantly prolonged the reaction time of treated mice to thermal pain near to 150% (approximately 3-fold enhancement) after 120 minutes of treatment time compared to the untreated mice. To further investigate the antinociceptive activity of *A. scopariae*, the participation of opioid and adenosine receptor systems were studied. Naxalone (2 mg/kg) which is an opioid receptor antagonist, completely compromised the antinociceptive effect of *A. scopariae*. This suggested that *A. scopariae* has significant pharmacological influence on the opioid receptor system. The participation of adenosine receptor in the antinociceptive activity of *A. scopariae* was evaluated using caffeine (10 mg/kg) as the antagonist of adenosine receptor. Pretreatment of caffeine significantly suppresses the antinociceptive effect of *A. scopariae*, suggesting the thermal antinociceptive effect of *A. scopariae* may have direct or indirectly agonize the adenosine receptors (Habib and Waheed, 2013).

2.2.3 Antipyretic Activity

Pyrexia is secondary conditions arise from infection, tissue damage, malignancy and graft rejection. The increase in the pro-inflammatory mediators such as interleukin 1 and tumor necrosis factor alpha cause the hypothalamus to increase

the body temperature by enhancing the production of prostaglandin. Antipyretic activity referred as the inhibitory effect in the production and release of prostaglandins. *A. scopariae* (800 mg/kg) reduced the yeast induced pyrexia in mice by 89.6% at 180 minutes post-administration. *A. scopariae* suppresses the synthesis and release of prostaglandins and subsequently lead to the reduction in body temperature. The high amount of artemisinin in *A. scopariae* contributes to its antipyretic activity (Habib and Waheed, 2012).

2.2.4 Antioxidant Activity

Singh et al. (2009) reported that the oil from the young and mature leaves of *A. scopariae* exhibited higher DPPH radical scavenging activity. The essential oil from mature leaves of *A. scopariae* exhibited stronger radical scavenging activity approximately 32 to 64% as compared to the essential oil from young leaves which is 18 to 71%. The IC_{50} value of mature leaf oil was 65.9 µg/mL, whereas the IC_{50} value of young leaf oil was 119.3 µg/mL, and it was appreciably lower than that of widely used antioxidant butylated hydroxytoluene (BHT) (140.6 µg/mL).

The hydroxyl radical scavenging activity of the oil from young and mature leaves of *A. scopariae* showed an excellent antioxidant activity with IC_{50} of 126.15 and 109.75 µg/mL, respectively. The antioxidant activity of the essential oil increases in a concentration dependent manner. The oil from young leaves of *A. scopariae* exhibited approximately 70% hydroxyl radical scavenging activity,

whereas mature leaves of *A. scopariae* recorded approximately 77% radical scavenging activity (Singh et al., 2009).

Hydrogen peroxide (H_2O_2) is very toxic when it penetrates into the cell membranes and causes the oxidation of cellular compounds. The H_2O_2 scavenging activity of both the young and mature leaves of *A. scopariae* were within the range of 11 to 59% and indicates a higher antioxidant activity. The IC_{50} for H_2O_2 scavenging activity from the oil of young and mature leaves were recorded at 170.11 and 153.95 µg/mL, respectively (Singh et al., 2009).

2.2.5 Anticancer Activity

A. scopariae extract was investigated for anticancer activity towards ER-a-positive T47D and ER-a-negative HS578T breast cancer cell lines. In T47D cells, different concentrations of extract ranging from 5 to 200 mg/mL at different period of times, namely 24, 48 and 72 hours showed a biphasic response. The extract enhanced the growth of T47D cells with lower concentrations (>100 mg/mL) and relatively short exposure time. When T47D cells were exposed to higher concentration of extract, the inhibition of proliferation enhanced significantly. At 200 mg/mL, the extract suppress the growth significantly by 38 to 66% as compared to negative control. In the case of HS578T cells, the extract showed weaker anticancer activities. Significant of cell proliferation inhibition only could be observed at the concentration of 200 mg/mL at 72 hours (Choi et al., 2013).

2.3 Silver Nanoparticles

Silver nanoparticles are nanoparticles of silver with size ranging from 1 to 100 nm (Prabhu and Paulosee, 2012). Silver nanoparticles have drawn the attention of researchers to explore new dimensions for their beneficial value due to their corresponding tiny size (Ahmed et al., 2016). Silver nanoparticles have been used in diverse fields such as medical, food, health care and industrial areas owing to their unique physicochemical properties. Silver nanoparticles also possess excellent biological activities such as antifungal, antioxidant, antibacterial and anti-inflammatory. Silver nanoparticles have been used as anticancer agents as well (He et al., 2017; Zhang et al., 2016).

Researchers reported that the silver nanoparticles were able to kill cancer cells by inducing apoptosis. Furthermore, a synergistic effect on the apoptosis was noted using uracil phosphoribosyltransferease (UPRT)-expressing cells and cells that are not UPRT with the use of fluorouracil (5-FU). In this research, silver nanoparticles not only play the role in inducing the apoptosis of cancer cells, it also sensitize the cancer cells toward chemotherapeutic drugs. Silver nanoparticles caused alterations in cell morphology, reduced cell viability and metabolic activity and enhanced the oxidative stress level in the cell which would eventually led to mitochondrial damage and enhanced the production of reactive oxygen species, and finally causing DNA damage to the cancer cells (Zhang et al., 2016).

Researchers also shown that chitosan-based nanocarrier delivery of silver nanoparticles causes apoptosis of cancer at very low concentrations. The nanocarrier with silver nanoparticles showed a greater inhibition compared to silver nanoparticles alone. Chitosan-coated silver nanoparticles were able to be taken up by human embryonic cells more efficiently. Plant mediated synthesis of silver nanoparticles exhibited higher significant toxic effect in human lung carcinoma, MCF7 and T47D cells as compared to non-cancer cells such as normal human lung cells and normal breast cell line (Zhang et al., 2016).

Silver is inert in human body but ionizes with the presence of moisture, body fluids, and secretions leading to the release of the Ag^+ ion that is biologically active. THE reduced ions exhibit a strong affinity for sulphydryl groups and cell membranes. The ionization of silver is proportional to the particles' surface area. Thus, the release of Ag^+ ion from nanocrystalline silver that is less than 20 nm is much higher than that from silver which is in other metallic forms. Studies have proved that nanocrystalline silver with greater solubility in water shows greater growth reduction in *Pseudomonas aeruginosa*. Ag^+ ions are able to interact with the protein residues on the cell membrane of bacteria, fungi and protozoa, subsequently being absorbed into the cell through pinocytosis. The presence of Ag^+ in the cell will cause protein denaturation and inactivation, including the enzyme such as RNAses and DNAses. This shows that silver can act as a potential antimicrobial agent. Based on previous studies, 60 ppm of Ag^+ is enough to control the bacterial and fungal growth (Lansdown, 2010).

2.4 Toxicity of Silver Nanoparticles

Individuals who are working with the production of silver over a long period have increased risk of argyria and argyrosis unless strict safety precautions such as using of air filters and personal respirators are implemented (Lansdown, 2010).

Specific toxicity investigations and clinical trials have been carried out in relation to wound dressings such as Acticoat which contain silver nanoparticles. Patients were exposed with acticoat for nine days showed an increment in blood silver (56.8 µg/L). After six months, the blood silver only normalized to 0.8 µg/L. Clinical studies are important in order to examine the occupational risks related to the use of silver nanoparticles that is highly dispersed in biocide, consumer products and chemical catalysis (Lansdown, 2010).

Laboratory examinations of the toxicity of silver nanoparticles are very few. Silver is taken up into cultured cells through pinocytosis and precipitate proteins in cytoplasm causing the cell death. Cultured cells treated with silver particles at 6.25 to 50 µg/mL exhibited changes in cell shape, sign of oxidative stress and enhanced lipid peroxidation. Inhalation toxicity studies in rat by Samsung Electronics Co. (Korea) reported that the lungs and liver are main target sites of silver nanoparticles but there were no observable effects at environmental concentrations of 100 mg/m^3. Exposure to silver nanoparticles at concentrations of 133 mg/m^3 or 515 mg/m^3 caused the lung to undergo inflammation and granulomatous changes and also bile duct hyperplasia (Lansdown, 2010).

2.5 Synthesis of Silver Nanoparticles

Silver nanoparticles are commonly synthesized through chemical and physical methods which can cause hazard to the environment due to the usage of toxic and perilous chemicals. The advancement of biologically-inspired experimental procedure for the synthesis of nanoparticles is becoming an essential branch of nanotechnology. There are two ways to synthesize silver nanoparticles namely "top to bottom" or "bottom to up" methods. In bottom to top method, chemical and biological methods are employed to synthesis the nanoparticles through the self-assemble of atoms into new nuclei, which may grow into a nanoscale particle. In the case of top to bottom, an appropriate bulk material is broken down into tiny particles through size reduction with different lithographic technique such as milling and grinding (Ahmed et al., 2016).

2.5.1 Chemical Method

Chemical reduction is the most widely used method to synthesize silver nanoparticles. Organic and inorganic reducing agents, such as sodium citrate, Tollen's reagent, ascorbate and elemental hydrogen are utilized to reduce silver ions (Ag^{+}) in aqueous solutions. In order to stabilize the nanoparticles, capping agents are used. The benefits of this approach is that a huge quantity of nanoparticles can be produced in a short time, ease of production and low cost (Ahmed et al., 2016). The disadvantages is the production of toxic chemical as the by products that are being released to the environment, and not highly purified products due to the surface of the nanoparticles are covered with chemical reductants (Zhang et al., 2016).

2.5.2 Physical Method

In this approach, nanoparticles are commonly synthesized by evaporation-condensation via a tube furnace at atmospheric pressure. The foundation material placed at the center of the furnace is vaporized into carrier gas. Silver, gold and fullerene nanoparticles have been synthesized previously through evaporation-condensation technique. Conventional physical methods such as spark discharging and pyrolysis were employed to synthesize silver nanoparticles. The advantages of this method are rapid, radiation used as reducing agent and no toxic chemicals involved. However, this method has several drawbacks too such as occupying large space occupying, consumption of high electrical power and long pre-heating time to attain suitable operating temperature. The main disadvantage is the surface structure of the product is imperfect and the physical properties of nanoparticles are greatly relies on the surface structure (Ahmed et al., 2016; Zhang et al., 2016).

2.5.3 Biological Method

In order to overcome the disadvantages of chemical and physical methods, biological method have become a reasonable choice to synthesize silver nanoparticles. Biological method is easy to use, cost effective and environmental friendly for the green synthesis of silver nanoparticles. Ag^+ ions are reduced and stabilized by a various biological systems including bacteria, fungi, plant extract and small biomolecules such as proteins, amino acids, tannins, phenolics and vitamins. The synthesis of nanoparticles are dependent on solvents, reducing agents and the non-toxic materials. Plants have drawn the attention of

researchers to synthesize nanoparticles due to its non-pathogenic, availability of secondary metabolites and removal of the extra step needed to avoid particle aggregation. The other advantages of biological method are ease in the control over shape, size and distribution of the synthesized nanoparticles, high density and ready solubility of synthesized nanoparticles in water (Ahmed et al., 2016; Zhang et al., 2016).

2.6 Characterization of Silver Nanoparticles

There are many methods in characterizing silver nanoparticles such as UV-Vis spectrophotometry, X-ray diffraction, Fourier transform infrared spectroscopy (FTIR) and scanning electron microscopy (SEM). However, thee research only uses UV-Vis spectrophotometry. UV-Vis spectroscopy is a widely used method in characterizing and controlling the stability of silver nanoparticles. Silver nanoparticles interact readily with specific wavelengths of light owing to their unique optical properties. On the other hand, UV-Vis spectroscopy is rapid, convenient, sensitive and selective for different types of nanoparticles, only require a short period of time for measurement and calibration is not needed for particle characterization on colloidal suspensions. In terms of silver nanoparticles, the conduction and valence bands are located in close proximity with each other in which electrons are free to move. These electron will then produce surface plasmon resonance (SPR) absorption band. This occurs because the electrons of silver nanoparticles undergo collective oscillation in resonance with the wave of light. The absorption of silver nanoparticles mainly relies on

the particle size, dielectric medium, and chemical environments (Zhang et al., 2016).

2.7 Antioxidant Assay

DPPH or α, α-diphenyl-β-picrylhydrazyl is one of the simple, cheap and widely used antioxidant assay. DPPH acts as a stable free radical to be scavenged by antioxidants. The odd electron of nitrogen atom found in DPPH is being reduced by accepting one hydrogen atom from the antioxidants. DPPH is considered as a stable free radical because of the delocalization of the free electron and no dimerization between molecules. Upon mixing DPPH solution with antioxidant, reduced and colorless form of DPPH will be formed and the reaction is as shown in **Figure 2.3**. DPPH radical is denoted by Z* and the donor molecule is represented by AH, the main reaction is as Z* + AH = ZH + A*. ZH is referred as the reduced form and A* is referred as the free radical generated in the first step. DPPH can be easily reduced by accepting an electron or hydrogen radical in reach stable state. DPPH exhibits a strong band at 517 nm caused by its odd electron and the solution is purple color, the absorption diminishes once the electron is paired (Kedara and Singh, 2011).

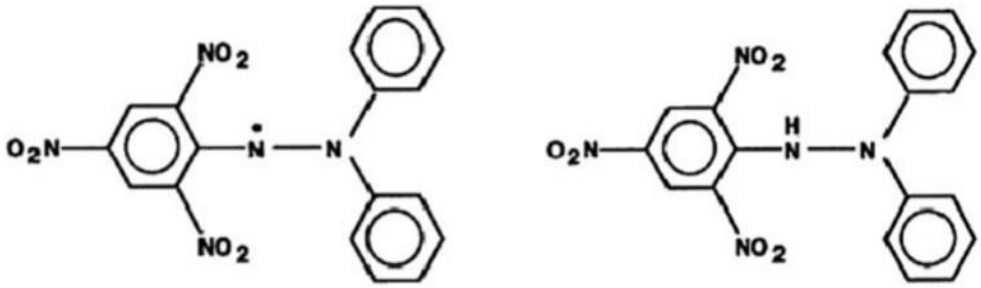

Figure 2.3: The chemical structure of DPPH (purple color) (left) and reduced form of DPPH (colorless) (right) (Adapted from Kedara and Singh, 2011).

2.8 Cytotoxic Assay

One of the most commonly used cytotoxic assay is thiazolyl blue tetrazolium bromide (MTT). MTT assay is considered as a very sensitive method to determine cell viability upon treatment. The MTT dye will only generate a very low background absorbance when there is no cells present. In this assay, the linear relationship of the viable cells with an active metabolism together with the color produced is established. This results in an accurate quantification of variation in the rate of cell death or growth. MTT is the widely used method in the screening of cytotoxicity of a drug. The principle of MTT assay is that the reduction of MTT reagent (yellow color) and other tetrazolium dyes bases on the cellular metabolic activities is due to the presence of NAD(P)H-dependent cellular oxidoreductase enzymes. The reduction reaction is as shown in **Figure 2.4**. Viable cells will yield a rapid reduction of MTT to formazan (purple color) that can be dissolved in dimethyl sulfoxide (DMSO). The formazan formed can be directly quantified at the wavelength of 540 nm which is directly proportional to the enzyme activity. High intensity of purple color means higher cell viability, yellow color intensity denotes the decreased cell number and thus the cytotoxicity of the test substance (Bahuguna et al., 2017).

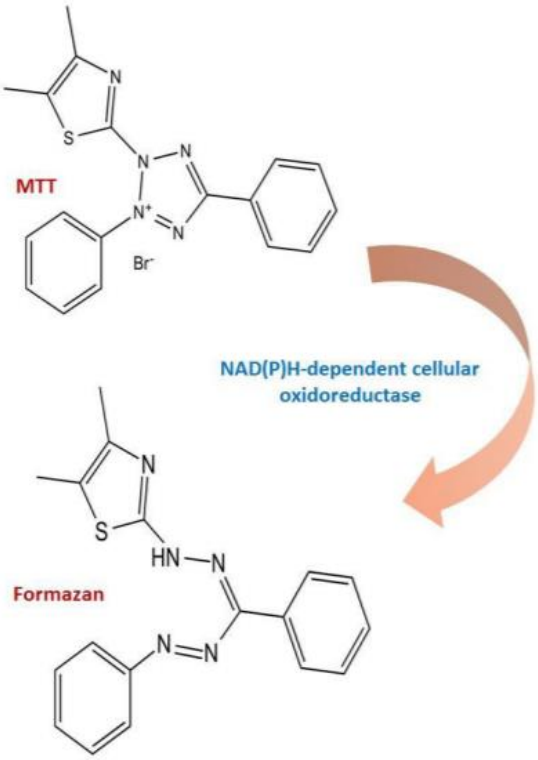

Figure 2.4: The formation of formazan by NAD(P)H-dependent cellular oxidoreductase (Adapted from Bahuguna et al., 2017).

CHAPTER 3

MATERIALS AND METHODS

3.1 Materials

3.1.1 Plant Source

Approximately 500 g of *Artemisiae scopariae* was purchased from Sun Meng Hong Sdn Bhd, Ipoh and authenticated by the dealer itself.

3.1.2 Cancer Cell Lines

Human cervical adenocarcinoma (HeLa) (ATCC® CCL-2™) and human colon adenocarcinoma (HT-29) (ATCC®HTB-38™) were used in this research. The cryopreserved cell lines were cultured in Dulbecco's Modified Eagle Medium (DMEM) with 10% of fetal bovine serum. The cells were observed periodically under inverted phase contrast microscope.

3.1.3 Reagents, Chemicals, Equipment and Laboratory Wares

Reagents and chemicals used in this research were listed in **Table 3.1**, whereas the equipment used were listed in **Table 3.2**.

Table 3.1: List of reagents and chemicals used with respect to their brands or manufacturers.

Reagents and chemicals	**Brands/Manufacturers**
2,2-diphenyl-1-picrylhydrazyl (DPPH)	Sigma-Aldrich
Dimethyl sulfoxide	Bio Basic Canada Inc
Doxorubicin hydrochloride	Sigma-Aldrich
Dulbecco's Modified Eagle Medium	Biowest
Fetal bovine serum	Sigma-Aldrich
L-Ascorbic acid	Gene Chem
Methanol	Irama Canggih Sdn. Bhd.
MTT	EMD Millipore Corp.
Phosphate-buffered saline	Chem Solu
Silver nitrate	Bendosen
Thiazolyl blue tetrazolium bromide	Sigma-Aldrich
Trypan blue	Life Technologies

Table 3.2: List of equipment used with respect to their manufacturers.

Equipment and laboratory wares	Manufacturers
Freezer (-20°C)	Snow
Chiller (4°C)	Copen Scientific Sdn Bhd, SAMEMAX REFRIGERATION SDN BHD
Analytical balance	KERN, METTLER TOLEDO
Biological safety cabinet II	ESCO
CO_2 incubator	Binder
Drying oven	Memmert
Freeze dryer	Martin Christ, LaboGene
Hotplate stirrer	LMS Co., Ltd
Inverted microscope	Olympus Corporation
Laminar flow hood	ESCO
Multi-mode microplate reader	BMG LABTECH
Centrifuge	Thermo Scientific
Rotary shaker	N-BIOTEK
Sonicator	Thomas Scientific
UV-Vis spectrophotometer	GENESYS 10S
Vortex	Gemmy Industrial Corporation
Water bath	Memmert

3.2 Plant Extraction

The dried plant was blended to fine powder using a laboratory blender. The powdered sample was added with 1 L of deionized water and was boiled on a hotplate for 30 minutes. The mixture was continuously stirred during the boiling and was left to cool in room temperature. The mixture was filtered using cotton wool into a flask and kept in -20°C freezer overnight. The frozen sample was freeze dried using a freeze drier and the lyophilized sample was stored in -20°C freezer until further usage.

3.3 Synthesis of Silver Nanoparticles

The aqueous extract was filtered twice with Whatman no. 1 filter paper prior to the synthesis of silver nanoparticles (AgNPs). The filtrate was stored in 4°C chiller until further usage. Prior to the synthesis of silver nanoparticles, 200 mL of 1 mM of silver nitrate ($AgNO_3$) was prepared in dark. Approximately 33.97 mg of $AgNO_3$ powder was weighed and dissolved in 200 mL of deionized water. The $AgNO_3$ was prepared in a conical flask wrapped with aluminium foil. The solution was swirled to dissolve the powder completely. The solution was sealed and stored in 4°C chiller until further usage.

The filtrate and $AgNO_3$ were first brought to the room temperature before the synthesis of silver nanoparticles. To synthesize 100 mL of silver nanoparticles with a ratio of aqueous extract to $AgNO_3$ (1:9), 10 mL of the aqueous extract was added to 90 mL of $AgNO_3$ in a conical flask wrapped with aluminium foil. In order to optimize the optimum ratios of aqueous extract to $AgNO_3$, the synthesis

of silver nanoparticles was repeated with different ratios of aqueous extract to $AgNO_3$ which were 1:1 and 9:1. All the solutions were shaken constantly in a shaking incubator at 120 rpm at 25°C. The optimization of the absorption spectrum of all the solutions were performed at different time intervals which were 0.5 hour, 4 hours and 24 hours. After the measurement, the solutions were freeze dried and kept in -20°C freezer.

3.4 Characterization of Silver Nanoparticles

3.4.1 Color Changes

The color changes of the aqueous extract, different ratios of synthesized silver nanoparticles and $AgNO_3$ were observed at different time intervals such as 0.5 hour, 4 hours and 24 hours.

3.4.2 UV-Vis Spectrophotometer

A volume of 1 mL of AgNPs at ratio 1:9 was pipetted into Quartz cuvette and the absorbance was measured using UV-Vis spectrophotometer with deionized water as blank. The absorption spectrum of the solution was read in the range of 300 to 700 nm with the resolution of 1 nm. The absorbance of the AgNPs at ratio1:9 was recorded at different intervals which were 0.5 hour, 4 hours and 24 hours incubation. The measurement was repeated with other ratios of silver nanoparticles, aqueous extract and $AgNO_3$.

3.5 Antioxidant Assay

3.5.1 Preparation of Reagents and Samples

A concentration of 0.2 mM of DPPH reagent was prepared by dissolving 1.56 mg of DPPH in 20 mL of methanol and was incubated in dark at room temperature for 30 minutes. The reagent was wrapped with aluminium foil and kept at 4°C chiller until further usage.

Stock concentrations of 10 mg/mL of the AgNPs at ratio 1:9 were prepared by dissolving 10 mg of the freeze dried samples in 1 mL of deionized water. The preparation of stock solutions were repeated with aqueous extract, AgNPs at ratios 1:1 and 9:1. The stock solutions were wrapped with aluminium foil and stored at -20°C freezer.

Ascorbic acid of 5 mg/mL was prepared by dissolving 5 mg ascorbic acid in 1 mL of deionized water. The ascorbic acid was wrapped with aluminium foil and kept at -20°C freezer. Negative control used in this assay was methanol. Methanol was stored at room temperature.

3.5.2 DPPH Assay

DPPH assay was performed in a round-bottom of 96-well plate and 100 µL of methanol was firstly added to all the wells. A volume of 100 µL of various samples and ascorbic acid were added to Columns A3 to A12, respectively, as shown in **Figure 3.1.** These samples were serially diluted with methanol to concentration ranging from 0.02 to 2.50 mg/mL. About 20 µL of DPPH was

added to every wells and the plate was incubated in dark for 30 minutes. The absorbance was read using microplate reader at 517 nm. Graph of percentage of radical scavenging activity against concentration was plotted and EC_{50} value was determined from the graph. The percentage of radical scavenging activity was determined using the following formula (Reddy et al., 2014).

Percentage of radical scavenging activity = [(=Absorbance of control-absorbance of test) / absorbance of control] x 100

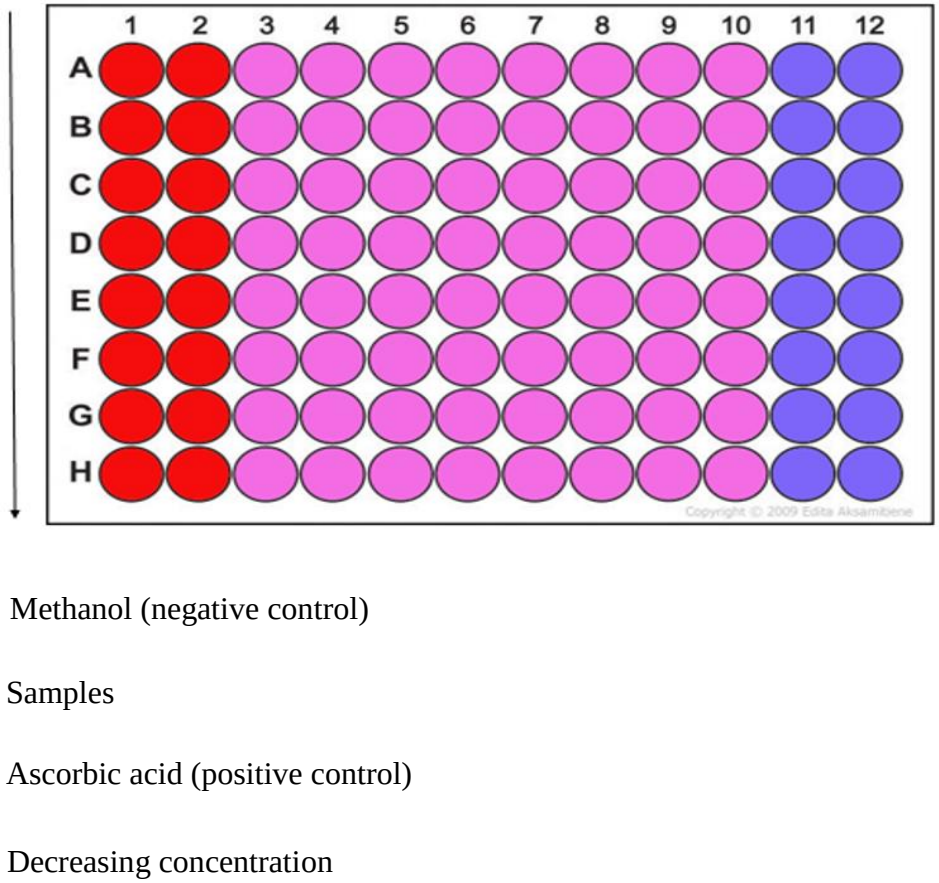

Figure 3.1: The experimental design of DPPH assay.

3.6 Cell Culture and Cytotoxic Assay

3.6.1 Preparation of Reagents, Medium and Chemicals

Complete medium was prepared by adding 10 mL of fetal bovine serum into 90 mL of basic DMEM. Phosphate buffered saline was prepared by adding two tablets of phosphate buffered saline (PBS) into 200 mL of deionized water. The PBS was autoclaved at 121°C for 20 minutes at 15 psi of pressure. The complete medium and PBS were tested for sterility by adding 2 mL of the respective samples to the petri dish. The petri dishes were incubated overnight at 37°C in humidified 5% CO_2 incubator. The petri dishes were checked for any contaminants using inverted microscope the following day. The PBS and DMEM were sealed and kept at 4°C chiller.

A concentration of 5 mg/mL of MTT reagent was prepared by adding 100 mg of MTT powder to 20 mL of phosphate buffer saline. The reagent was first vortexed and then filtered using 0.22 µm nylon filter into a centrifuge tube. The MTT reagent was wrapped with aluminium foil and kept at -20°C freezer.

Doxorubicin hydrochloride was used as positive control and 1 mg/mL of working solution was prepared by adding 100 µL of doxorubicin hydrochloride to 900 µL of basic DMEM. These solutions were sealed and kept at -20°C freezer.

3.6.2 Culture and Subculture of Cells

HeLa and HT-29 cancer cell lines were taken out from liquid nitrogen tank. The cell lines were thawed immediately in water bath at 37°C for one minute. About 1 mL of cells were pipetted into a 25 cm^3 culture flasks filled with 4.5 mL of complete medium. The flasks were observed under inverted microscope and incubated at 37°C in humidified 5% CO_2 incubator for 24 hours. After 24 hours, the cells were observed for any attachment under inverted microscope. For attached cells, the medium was changed by removing the old medium and adding in 5 mL of new complete medium. For floating cells, the cell suspension was transferred into a centrifuge tube, sealed with parafilm and centrifuged for 6 minutes at 1000 rpm. The supernatant was removed and the cell suspension was resuspended with DMEM. The cell suspension was cultured into a new 25 cm^3 culture flask containing 5 mL of complete medium. The cell culture flask was further incubated at 37°C in humidified 5% CO_2 incubator.

Once the cells reached 80 to 90% confluency, subcultured was performed by transferring 2 mL of cell suspension from the old flask to the new flask. Approximately 2 mL of complete medium was added to the old flask and the new flask. The cells in both flasks were observed under inverted microscope and then incubated at 37°C in humidified 5% CO_2 incubator.

3.6.3 Preparation of Samples

A stock concentration of AgNPs at ratio 1:9 was prepared by adding 10 mg of freeze dried sample to 2 mL of sterile deionized water to obtain a concentration of 5 mg/mL. The working concentration of 1 mg/mL was prepared by diluting the stock solution with basic DMEM. The preparation of stock and working solutions were repeated with aqueous extract and AgNPs at ratio 1:1 and 9:1. These solutions were wrapped with aluminium foil and stored at -20°C freezer.

3.6.4 Cell Counting

The cells suspension was transferred to the centrifuge tube and centrifuged at 1000 rpm for 10 minutes. After centrifugation, the supernatant was removed and the pellet was resuspended with DMEM. A volume of 100 µL of cell suspension was mixed with 100 µL of trypan blue in an Eppendorf tube. The mixture was incubated in room temperature for three minutes. A volume of 20 µL of the mixture was loaded onto the hemocytometer. The hemocytometer was viewed under the inverted microscope. The average number of viable cells in four grids were calculated. The concentration of the cells was calculated by using the following formula (University of Queensland, 2017).

Concentration of cells= average number of viable cells x 1 x 10^4 x dilution factor x original volume of cell suspensions.

3.6.5 MTT Assay

MTT assay was performed using a treated 96-well plate (flat bottom). A volume of 50 µL of basic DMEM was added to every wells, followed by the addition of 50 µL of samples and doxorubicin hydrochloride in Columns A3 to A12, respectively, as shown in **Figure 3.2**. The samples were serially diluted with basic DMEM to the concentrations ranging from 3.91 to 500 µg/mL. A volume of 50 µL of cells suspension with the concentration of 1 x 10^4 cells per well were seeded to all the wells. The plates were sealed with parafilm and incubated at 37°C in humidified 5% CO_2 incubator. The plates were incubated for 24 and 48 hours, respectively. After incubation, 10 µL of MTT was added to all the wells. The cells were incubated in dark for 4 hours at 37°C in humidified 5% CO_2 incubator. About 100 µL of DMSO was added to the wells to dissolve the formazan crystal and was further incubated for 15 minutes. The absorbance was read at 550 nm using the microplate reader. Graph of percentage cell viability against concentration was plotted and IC_{50} value was determined from the graph. The percentage of cell viability was determined by using the following formula (Reddy et al., 2014).

Percentage of cell viability= (absorbance of test/ absorbance of control) x 100

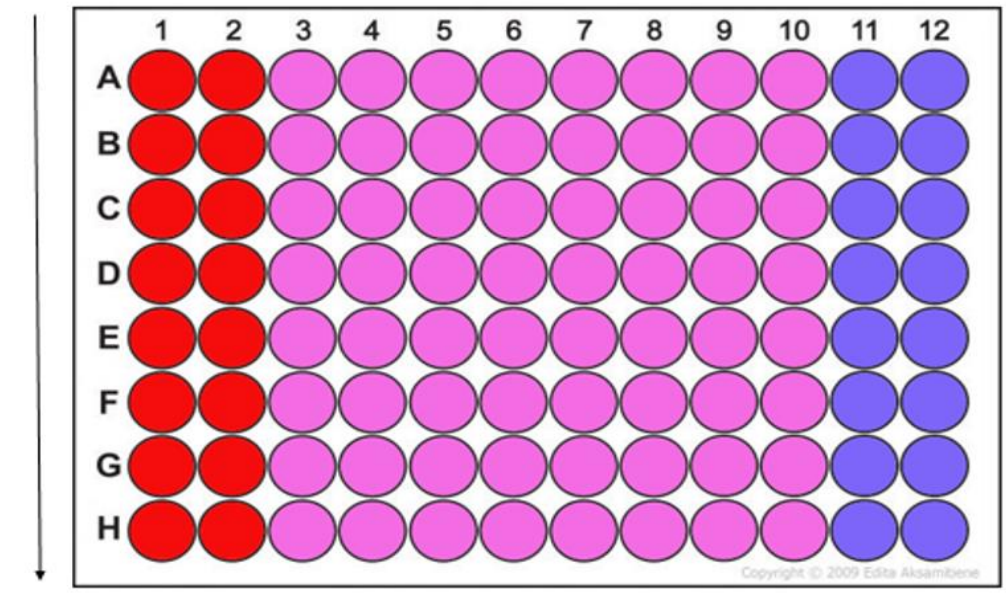

Figure 3.2: The experimental design of MTT assay.

3.7 Statistical Analysis

The DPPH assay was repeated thrice, whereas MTT assay was repeated twice. The data were expressed as mean ± standard deviation. Student *t*-tests were performed to express experimental significance of the results. The results with the *p*-value of <0.05 were considered as statistically significance.

CHAPTER 4

RESULTS

4.1 Percentage of Lyophilized Yield

The dried weight of *A. scopariae* used in the aqueous extraction was 514.32 g. The yield of the aqueous extract after freeze drying was 8.88% (45.67 g). The weight of synthesized silver nanoparticles (AgNPs) at ratios of 1:1, 1:9 and 9:1 were 2.41 g, 0.15 g and 12.29 g, respectively. Among the synthesized silver nanoparticles, 9:1 ratio showed the highest yield of 2.39%, while 1:1 ratio showed 0.47%. Silver nanoparticles at ratio 1:9 showed the least yield of 0.03%. The percentage of yield in different ratios of silver nanoparticles is as shown in **Figure 4.1**.

4.2 Characterization of Silver Nanoparticles

4.2.1 Color Changes

The color changes of the samples before and after synthesis of AgNPs were shown in **Figure 4.2**. The color changes of the solutions from darker brown to reddish brown shows the formation of silver nanoparticles. On the other hand, the color of the aqueous extract and $AgNO_3$ remained the same.

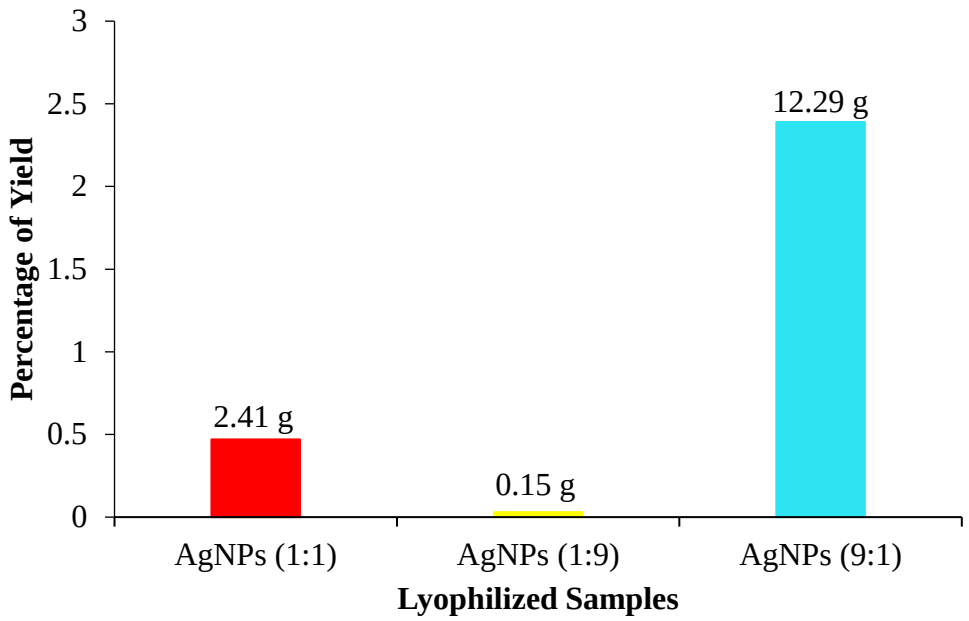

Figure 4.1: The yield of different ratios of silver nanoparticles.

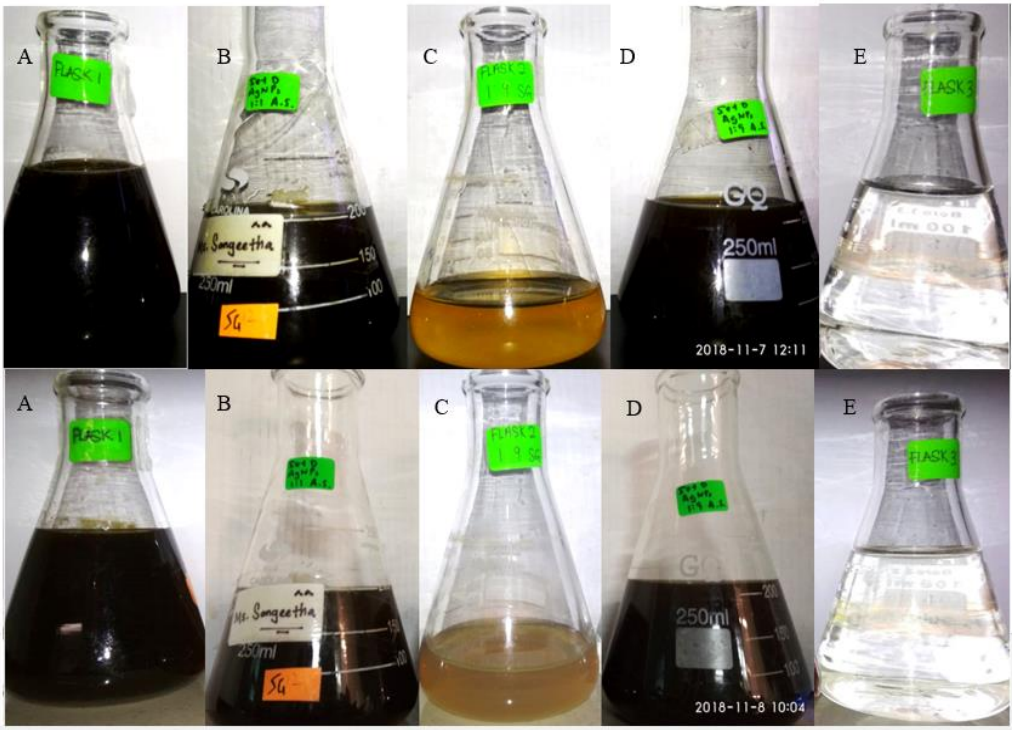

Figure 4.2: The color changes of samples after 24 hours synthesis. The color changes observed before (top) and after (bottom) in the synthesis of silver nanoparticles. (A) Aqueous extract; (B), (C) and (D) are silver nanoparticles at 1:1, 1:9 and 9:1 ratios, respectively; (E) silver nitrate.

4.2.2 UV-Vis Spectrophotometry

The absorption spectrum of the aqueous extract, silver nitrate and different ratios of AgNPs were measured at wavelength ranging from 300 to 700 nm using UV-Vis spectrophotometer. The absorption spectra is as shown in **Figure 4.3**. The absorption peak of aqueous extract was observed at 350 nm. Whereas for the AgNPs at ratios of 1:1, 1:9 and 9:1, the absorption peaks were observed at 400, 325 and 455 nm, respectively. Among the silver nanoparticles, the absorption peak of AgNPs at ratio 9:1 was broader with longest wavelength, whereas AgNPs at ratio 1:9 exhibited sharper peak with shortest wavelength. No absorption band was observed in silver nitrate.

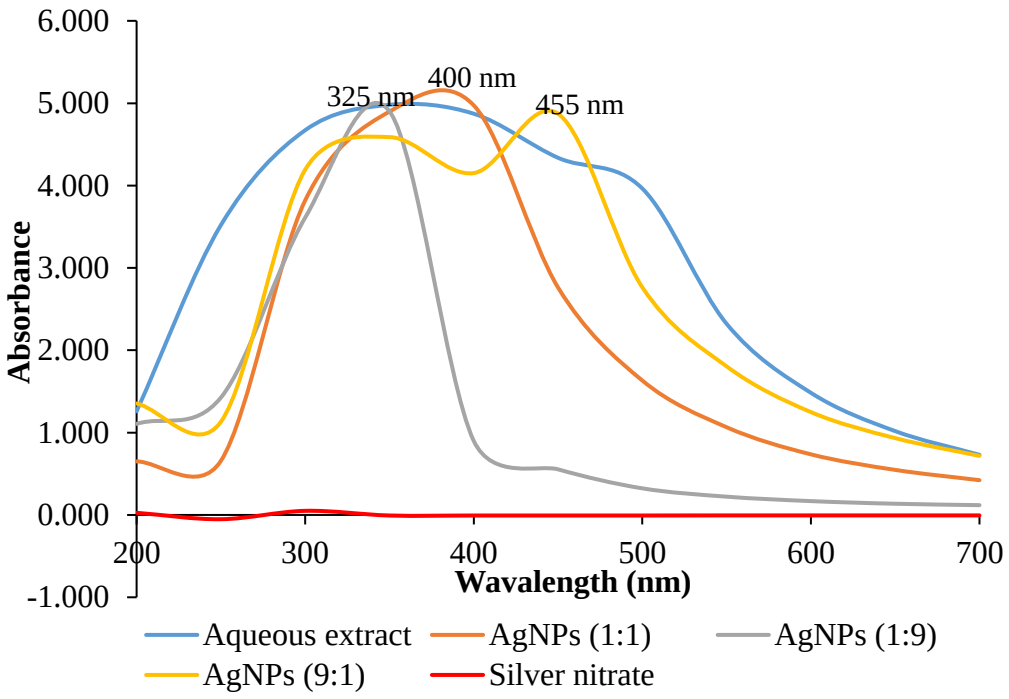

Figure 4.3: The absorption spectrum of the aqueous extract, silver nitrate and synthesized silver nanoparticles

4.3 DPPH Assay

The percentage of radical scavenging activity was calculated and tabulated in **Table 4.1**. Among all the samples, AgNPs at ratio 9:1 exhibited highest radical scavenging activity of 75.3% at 0.02 mg/mL. AgNPs at ratio 1:9 showed the lowest radical scavenging activity of 11.8% at 0.63 mg/mL. Aqueous extract alone exhibited 74.7% of radical scavenging activity at 0.02 mg/mL. Meanwhile, AgNPs at ratio 1:1 showed 73.1% at 0.02 mg/mL. Ascorbic acid showed the highest radical scavenging activity with 76.9% at 0.02 mg/mL.

Figure 4.4 shows the trend in the radical scavenging activity of aqueous extract, different ratios of silver nanoparticles and ascorbic acid at different concentrations. The antioxidant activity of the aqueous extract and silver nanoparticles decreased slightly as the concentration increased. In AgNPs at ratio 1:9, a sharp drop of radical scavenging activity was observed from concentration of 0.04 to 0.08 mg/mL. Meanwhile, a steady trend of higher radical scavenging activity was observed in ascorbic acid at various concentrations.

Table 4.1: The percentage of radical scavenging activity of aqueous extract, silver nanoparticles and ascorbic acid.

Concentration (mg/mL)	Percentage of Radical Scavenging Activity				
	Extract	AgNPs (1:1)	AgNPs (1:9)	AgNPs (9:1)	Ascorbic acid
0.00	0.0 ± 0.000	0.0± 0.000	0.0± 0.000	0.0 ± 0.000	0.0 ± 0.000
0.02	74.7± 0.004	73.1± 0.007	67.0± 0.004	75.3± 0.005	76.9± 0.013
0.04	72.2± 0.002	69.9± 0.004	56.7± 0.015	71.4± 0.006	76.6± 0.002
0.08	70.9± 0.004	68.9± 0.007	27.0± 0.077	66.3± 0.012	74.0± 0.004
0.16	70.5± 0.002	64.1± 0.007	28.9± 0.027	66.5± 0.005	76.9± 0.003
0.31	63.9± 0.004	59.6± 0.006	24.9± 0.037	59.6± 0.010	75.2± 0.002
0.63	57.9± 0.004	37.8± 0.033	11.8± 0.000	45.2± 0.030	72.5± 0.004

Data are expressed as means ± standard deviation (SD) (n=3) and significant at $p<0.05$ (Student t-test).

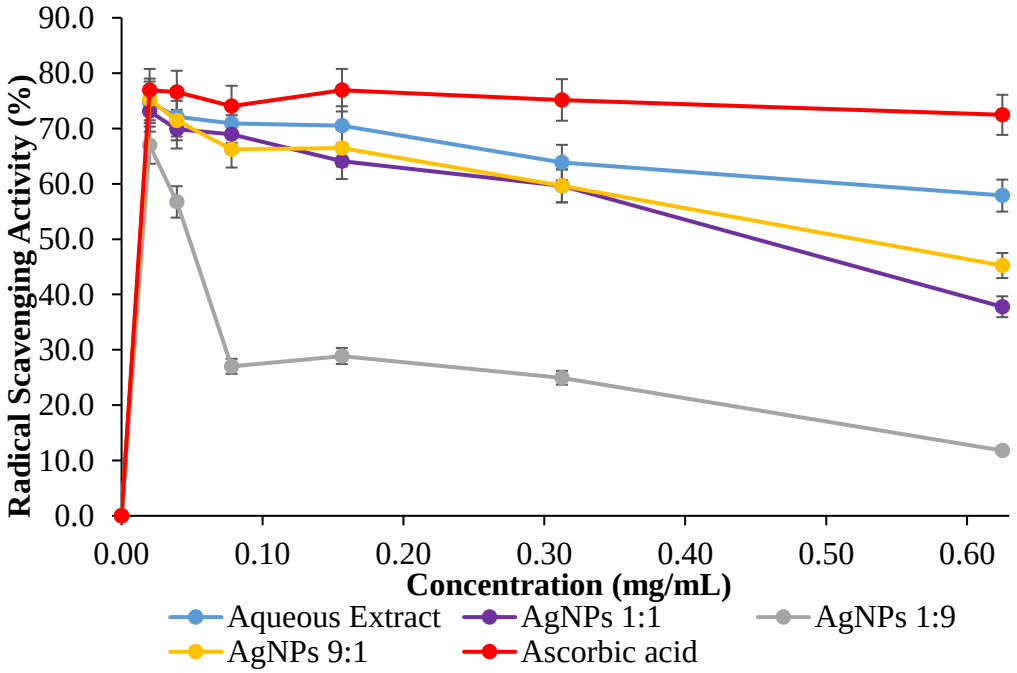

Figure 4.4: The percentage of radical scavenging activity of samples and ascorbic acid at various concentrations.

The EC_{50} values of the aqueous extract, different ratios of silver nanoparticles and the ascorbic acid were interpolated from graphs as shown in **Appendix A (Figures A and B)**. The EC_{50} value is as shown in **Table 4.2**. There were no significant differences being observed in all the samples as the EC_{50} values were in the range of 0.013 to 0.015 mg/mL.

Table 4.2: The EC_{50} of the aqueous extract, different ratios of silver nanoparticles, and ascorbic acid.

Sample	**EC_{50} (mg/mL)**
Aqueous extract	0.013
AgNPs at ratio 1:1	0.014
AgNPs at ratio 1:9	0.015
AgNPs at ratio 9:1	0.013
Ascorbic acid	0.013

4.4 MTT Assay

4.4.1 HeLa Cells

The percentage cell viability of HeLa cells after 24 hours treated with aqueous extract, different ratios of silver nanoparticles and doxorubicin hydrochloride is as shown in **Table 4.3**. Overall, the percentage cell viability of HeLa cells treated with all the samples were in the range of 8 to 14%. All the samples showed higher cytotoxicity against HeLa cells. The highest of cell viability was observed in AgNPs at 9:1 with 13.5% at 125 µg/mL. Aqueous extract exhibited the lowest cell viability of 8.5% at 7.81 µg/mL. Meanwhile, AgNPs at ratio 1:1 showed cell viability of 8.9% at 7.81 µg/mL.

Table 4.3: The percentage of cell viability of HeLa cells after 24 hours treatment with samples and doxorubicin hydrochloride.

Samples	Concentrations (µg/mL)	Cell viability (%)
Aqueous extract	0.00	100.0±0.000
	3.91	8.8±0.007
	7.81	8.5±0.029
	15.63	8.8±0.024
	31.25	9.1±0.014
	62.50	10.6±0.009
	125.00	11.5±0.034
AgNPs (1:1)	0.00	100.0±0.000
	3.91	9.1±0.025
	7.81	8.9±0.028
	15.63	9.2±0.031
	31.25	9.4±0.047
	62.50	10.5±0.022
	125.00	11.5±0.030
AgNPs (1:9)	0.00	100.0±0.000
	3.91	8.8±0.030
	7.81	9.0±0.038
	15.63	9.0±0.021
	31.25	9.5±0.026
	62.50	10.3±0.033
	125.00	12.4±0.020
AgNPs (9:1)	0.00	100.0±0.000
	3.91	8.9±0.032
	7.81	9.5±0.030
	15.63	9.3±0.022
	31.25	10.0±0.031
	62.50	10.8±0.050
	125.00	13.5±0.043

Table 4.3: Continued.

Samples	Concentrations (µg/mL)	Cell viability (%)
Doxorubicin hydrochloride	0.00	100.0±0.000
	3.91	9.2±0.037
	7.81	9.5±0.033
	15.63	9.9±0.028
	31.25	10.0±0.038
	62.50	10.6±0.045
	125.00	13.0±0.067

Data expressed as means ± standard deviation (SD) (n=2) and significant at $p<0.05$ (student t-test).

Figure 4.5 shows the trend of percentage cell viability of HeLa cells treated with aqueous extract, different ratios of silver nanoparticles and doxorubicin hydrochloride. Overall, the percentage cell viability of HeLa cells decreases sharply after treatment and further becomes constant at increasing concentration. The same trend was observed for doxorubicin hydrochloride. The cells were killed after the treatment at 24 hours.

The IC_{50} values were interpolated from the graphs as shown in **Appendix B (Figures C and D)**. The IC_{50} values are as shown in **Table 4.4.** The highest IC_{50} value was observed in doxorubicin hydrochloride with 2.152 µg/mL. Meanwhile, aqueous extract and AgNPs (1:9) exhibited the lowest IC_{50} values of 2.144 µg/mL, respectively.

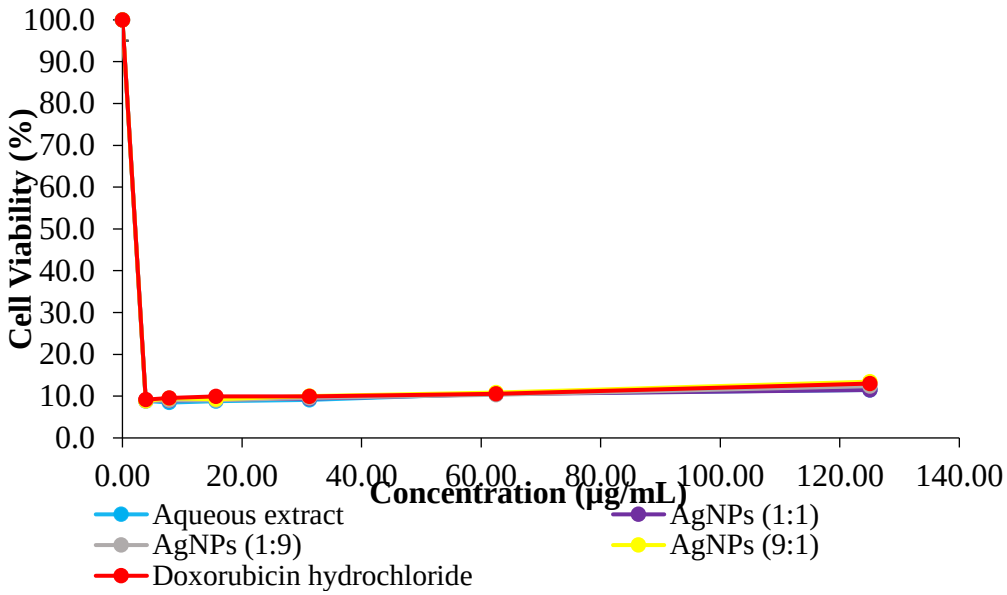

Figure 4.5: The percentage of cell viability of HeLa cells after 24 hours treatment with aqueous extract, different ratios of AgNPs, and doxorubicin hydrochloride at various concentrations.

Table 4.4: The IC_{50} of the aqueous extract, different ratios of silver nanoparticles and doxorubicin hydrochloride for HeLa cells.

Samples	**IC_{50} (µg/mL)**
Aqueous extract	2.144
AgNPs 1:1	2.150
AgNPs 1:9	2.144
AgNPs 9:1	2.145
Doxorubicin hydrochloride	2.152

4.4.2 HT-29 Cells

The percentage cell viability of HT-29 cells after 24 and 48 hours treatment with aqueous extract, different ratios of silver nanoparticles and doxorubicin hydrochloride are shown in **Table 4.5**. The highest and lowest cell viability after 24 hours treatment was observed in aqueous extract with 89.7% at 500 µg/mL and 31.1% at 3.91 µg/mL, respectively After 48 hours, aqueous extract still showed the highest cell viability of 63.1% at 500 µg/mL, however, the lowest cell viability was observed in AgNPs at ratio 1:1 of 28.3% at 7.81 µg/mL.

Figure 4.6 shows the trends in the cell viability of HT-29 cells after 24 hours treatment with different concentration of aqueous extract, silver nanoparticles and doxorubicin hydrochloride. All the treatments showed decreases and then increases in the percentage of cell viability as the concentration increases. Treatment with aqueous extract showed a sharp increase in percentage of cell viability from 250 to 500 µg/mL.

Figure 4.7 displays the percentage of cell viability of HT-29 cells after 48 hours treatment with of aqueous extract, various ratios of silver nanoparticles and doxorubicin hydrochloride at different concentration. All the treatments showed slight increase in the percentage of cell viability as the concentration increases.

Table 4.5: The percentage cell viability of HT-29 cells after 24 and 48 hours treatment with samples and doxorubicin hydrochloride.

Samples	Concentrations (µg/mL)	Cell viability (%)	
		24 hours	48 hours
Aqueous extract	0.00	100.0±0.000	100.0±0.000
	3.91	31.1±0.024	31.1±0.029
	7.81	33.4±0.001	29.0±0.015
	15.63	34.7±0.006	29.5±0.020
	31.25	38.1±0.024	31.6±0.024
	62.50	42.2±0.031	33.3±0.014
	125.00	50.0±0.008	36.8±0.014
	250.00	73.2±0.373	51.4±0.155
	500.00	89.7±0.338	63.1±0.236
AgNPs (1:1)	0.00	100.0±0.000	100.0±0.000
	3.91	32.2±0.015	28.8±0.014
	7.81	32.9±0.003	28.3±0.011
	15.63	35.0±0.009	29.1±0.009
	31.25	37.9±0.010	30.6±0.011
	62.50	42.6±0.005	33.1±0.023
	125.00	50.1±0.015	36.4±0.017
	250.00	56.7±0.019	41.6±0.015
	500.00	64.1±0.037	47.8±0.037

Table 4.5: Continued.

Samples	Concentrations (µg/mL)	Cell viability (%)	
		24 hours	48 hours
AgNPs (1:9)	0.00	100.0±0.000	100.0±0.000
	3.91	32.0±0.011	29.4±0.010
	7.81	33.4±0.003	29.0±0.008
	15.63	34.6±0.009	29.9±0.003
	31.25	36.9±0.006	30.2±0.002
	62.50	41.6±0.004	32.8±0.008
	125.00	48.0±0.010	35.0±0.010
	250.00	54.2±0.022	40.2±0.013
	500.00	65.9±0.052	47.7±0.021
Doxorubicin hydrochloride	0.00	100.0±0.000	100.0±0.000
	3.91	32.9±0.020	35.6±0.078
	7.81	33.2±0.018	35.9±0.074
	15.63	33.4±0.013	36.2±0.069
	31.25	35.0±0.017	36.8±0.062
	62.50	39.0±0.012	38.3±0.042
	125.00	47.2±0.015	41.6±0.002
	250.00	53.9±0.021	47.3±0.080
	500.00	67.1±0.043	48.1±0.086

Data expressed as means ± standard deviation (SD) (n=2) and significant at $p<0.05$ (student t-test).AgNPs at ratio 1:9 was not tested due to limited yield.

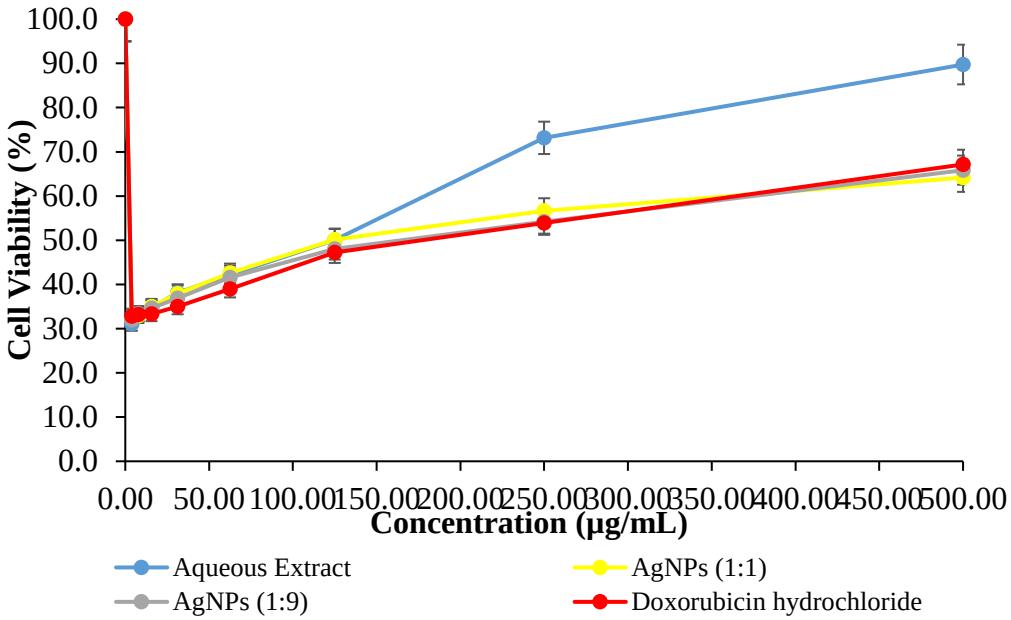

Figure 4.6: The percentage cell viability of HT-29 cells treated with aqueous extract, different ratios of AgNPs and doxorubicin hydrochloride at 24 hours.

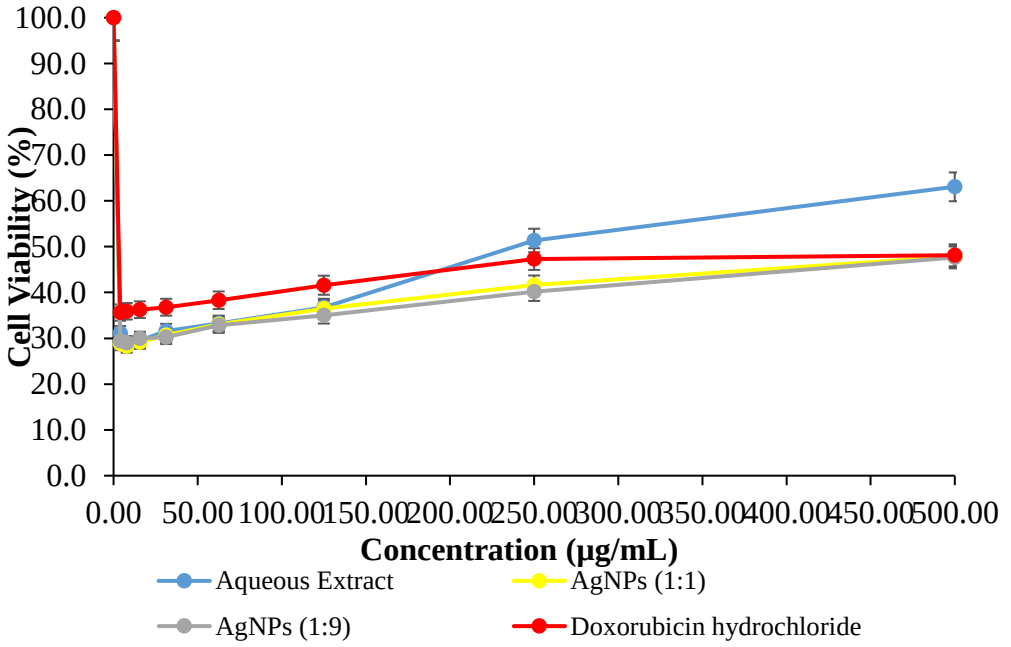

Figure 4.7: The percentage cell viability of HT-29 cells treated with aqueous extract, different ratios of AgNPs and doxorubicin hydrochloride at 48 hours.

The IC_{50} values were interpolated from the graphs as shown in **Appendix B (Figures E and F)**. The IC_{50} values are as shown in **Table 4.6**. The highest IC_{50} value was observed in doxorubicin hydrochloride with 2.912 µg/mL, whereas the lowest IC_{50} value was displayed by aqueous extract with 2.836 µg/mL at 24 hours. Meanwhile, at 48 hours, the highest IC_{50} value was exhibited by doxorubicin hydrochloride of 3.036 µg/mL, whereas the lowest IC_{50} value was shown by AgNPs at ratio 1:1 with 2.747 µg/mL.

Table 4.6: The IC_{50} of the aqueous extract, different ratios of silver nanoparticles and doxorubicin hydrochloride for HT-29 cells.

Samples	**IC_{50} (µg/mL)**	
	24 hours	**48 hours**
Aqueous extract	2.836	2.838
AgNPs (1:1)	2.885	2.747
AgNPs (1:9)	2.873	2.769
Doxorubicin hydrochloride	2.912	3.036

CHAPTER 5

DISCUSSION

5.1 Lyophilization Yield

Freezing was performed for aqueous extract of *A.scopariae* to obtain lyophilized sample. The process involve freezing of sample below its eutectic point, which is the minimum temperature at which the solid and liquid states of the sample coexist. The process ensures sublimation instead of melting in the subsequent process. Freeze drying process are divided to primary and secondary drying. In primary drying, the pressure is lowered and sufficient heat is applied to the sample to sublimate the water. In this initial drying step, approximately 95% of water in the sample is sublimated. The water sublimation in this step contributes greatly to the weight reduction of the aqueous extract and silver nanoparticles (AgNPs). On the other hand, in secondary drying, the water molecules that are not frozen will be removed. At this stage, the final water residue in the sample is ranging from 1 to 4% which is very low (Shukla, 2017). Therefore, these processes further confirm that the removal of water reduces the weight of the nanoparticles samples. Thus, leads to the lower percentage of yield of the samples in the range of 0.03 to 8.88% only in this research.

The appearance of freeze dried samples in this experiment were very sticky due to the nature of the sample which can be either hygroscopic or hydrophilic. The

lyophilized samples tend to reabsorb the moisture quickly from surrounding and causes stickness. Thus, storing these samples in a low humidity is crucial to reduce the risk of degradation by moisture exposure (Abascal et al., 2005; Labconco Corporation, 2010).

5.2 UV-Vis Spectrophotometry

5.2.1 Color Changes

After the addition of aqueous extract to the silver nitrate solution ($AgNO_3$), the color of different ratios of AgNPs turned into reddish brown. However, aqueous extract and $AgNO_3$ remained the same color. The color changes occurred slowly during the incubation hours. A complete color change was observed after 4 hours of incubation where no further changes of color were observed. This show that all the silver salt had been reduced to AgNPs. The reduction of the silver salt to AgNPs was contributed by the reducing and capping agents such as flavonoids in *A. scopariae.* The color changes are attributable to the chemical reduction of silver ions (Ag^+) to a silver atom (Ag). Many researchers also observed the reddish brown color changes although the plant extracts were different. UV-Vis spectrophotometer was used to observe the reduction of Ag^+ ions to Ag atoms. The AgNPs synthesized were reddish brown color in solution because of the excitation of surface plasmon resonance (SPR). Due to the changes in molecule and structure, the color transitions in AgNPs give rise to its corresponding variation in the light absorption ability in the visible wavelength of the electromagnetic spectrum. The SPR is due to the conduction of free electrons

through the induction of light (Rajendran et al., 2015; Kumar et al., 2017; Roy et al., 2017).

5.2.2 Absorption Spectrum

The aqueous extract of *A. scopariae* showed SPR band with broader range of wavelengths. This is due to the presence of phytochemicals in the plant extract and was detected in the range of spectrophotometry (Ramteke, 2013; Aziz et al., 2017). On the other hand, there was no SPR being observed in $AgNO_3$. This is due to the absence of reduction process of Ag^+ to Ag atom which will produce SPR band. Metal nanoparticles show a strong electromagnetic waves in the visible range due to the SPR. The SPR phenomenon happens due to the collective oscillations of the conduction electrons when visible light is irradiated on nanoparticles (Amin et al., 2012).

The SPR bands of the synthesized AgNPs at ratios 1:1, 1:9 and 9:1 appeared at 400, 325 and 455 nm, respectively. Among these, AgNPs at ratio 9:1 exhibited a broader SPR with the longest wavelength, followed by AgNPs at ratio 1:9 which had sharper SPR with shorter wavelength, and AgNPs at ratio 1:9 shown the sharpest SPR and shortest wavelength. A broad peak with longer wavelength reflects the increase in particle size, whereas the sharper band in a shorter wavelength indicates the smaller particle size (Shaik et al., 2018). The increment in particle size, the peak broadening, and the peak absorbance are due to the poly-dispersed nature of the particle with no sedimentation (Moosa et al., 2015). The wavelength of the AgNPs increased from 1:9 to 9:1 ratios and this implies

closely to the size of AgNPs. At higher extract ratio, the amount of reductants (electron-rich phytomolecules) present in the colloidal solution causes the reduction of Ag^+ becomes very fast. The presence of more functional groups in the plant extract facilitates the formation of more AgNPs due to the availability of more reduction sites. The rapid reduction of Ag^+ ions commonly mediates the growth of nanoparticles through a phenomenon known as Ostwald ripening which causes the size of AgNPs to increase. This eventually results in the large shift of the SPR band towards a longer wavelength and indicates the formation of large AgNPs. This further concludes that among the synthesized AgNPs, 9:1 ratio was the largest in size, followed by 1:1, and the smallest nanoparticles was the AgNPs at ratio 1:9 (Moosa et al., 2015; Shaik et al., 2018).

5.3 DPPH Assay

Reactive oxygen species (ROS) consists of singlet oxygen, superoxide ion, hydroxyl ions and hydrogen peroxide. These ROS are very reactive and toxic molecules formed in cells during metabolism. However, the production of ROS may increase due to pollutants, tobacco smoke, solvent and alcohol consumption. ROS can act as the source of oxidative damage to the proteins, lipids and DNA. ROS had been associated to the pathogenesis of some diseases such as cancer, asthma, diabetes and Parkinson's. Living cells have a great radical scavenging mechanism to prevent the production of excess ROS which then lead to cellular injury. The radical scavenging mechanism is performed by antioxidant. An antioxidant can be generally recognized as any substance that can delay or even inhibit oxidative damage to a biomolecule. The main role played by antioxidant

is the ability to trap free radicals. Antioxidant compounds such as phenolic acid, polyphenols and flavonoids are able to scavenge different types of free radicals. Herbal plants are good antioxidant source for human because the plants contain many phytochemicals that can act as antioxidant (Singh et al., 2009; Mahdi-Pour et al., 2012).

Based on the results, the aqueous extract and all the AgNPs possessed higher radical scavenging activity and almost similar to ascorbic acid. The highest radical scavenging activity was observed in AgNPs at ratio 9:1 with 75.3% and similar to that of ascorbic acid with 76.9%. The high radical scavenging activity can be due to the secondary metabolites as antioxidants work in a synergistic ways to enhance the radical scavenging activity. The radical scavenging activity varies as the concentration becomes higher. The variations is possibly due to the different amount of antioxidant found in different concentrations. The higher the amount of the antioxidant, the higher the radical scavenging activity (Marxen et al., 2007).The phytochemical such as polyphenols have strong antioxidant activity and the antioxidant activity was further enhanced through the conversion into AgNPs (Otunola et al., 2017). In contrast, lower radical scavenging activity was seen in AgNPs at ratio 1:1. The ceases of radical scavenging activity might be due to the antagonism activity of the antioxidants (Nambikkairaj and Thanighararassu, 2018). Antagonism and synergism occurs due to the variations in the chemical structure of the antioxidants. For instance, the oxidability of phenolic compounds relies on hydroxyl groups found in a benzene ring and also in the *ortho* effect of two hydroxyl groups together with carbonyl groups. The screening of hydroxyl groups gives rise to a significant increase in the efficiency

of antioxidants as compared to the unshielded phenol (Sazhina et al., 2018). The synthesized AgNPs may have the antioxidant property due to the presence of functional group as phenol or flavonoids on the surface of silver nanoparticles. These functional groups serve as the capping and stabilizing agent for the silver nanoparticles to exert its effects (Keshari et al., 2018).

Based on the literature review, *A. scopariae* may possibly contains both flavonoids and phenolic compounds. Flavonoids are widely found in vegetables, fruits, barks, roots and stems of plants. Flavonoids exhibit strong antioxidant activity by protecting the cells from free radical damages. Flavonoids are being oxidized by free radicals and transform the radicals become less reactive and more stable. Because of the great reactivity of the hydroxyl groups, the radicals are transformed into inactive state, based on the following equation: Flavonoid (OH) + R → flavonoid (O) + RH, where R indicates the free radical and O represents an oxygen free radical. Certain flavonoids act by directly scavenge superoxides, while other flavonoids have the ability to scavenge radicals that are highly oxygen-derived, known as peroxynitrite. Through the scavenging of free radicals, flavonoids are able to prevent LDL oxidation (Nijveldt et al., 2001).

Phenol consists of a benzene ring with one of its hydroxyl group being substituted by hydrogen atom (Adams et al., 2014). Phenolic compounds in *A.scopariae* are classified as secondary metabolites of the plant (Swanson, 2003). Phenolic has remarkable antioxidant activity by scavenging free radicals. Phenolic contains hydroxyl groups which are potential hydrogen donor. The antioxidants that can donate hydrogen can interact with ROS in a termination

reaction and terminate the cycle of production of new free radicals. The π-electrons in the benzene rings of the phenolic are able to produce free radicals where the radical is stabilized via delocalizations. The production of the long-lived radicals is capable of altering the radical-mediated oxidation process. The antioxidant property of phenolic is also contributed by the ability of chelate metal ions involved in the generation of free radicals (Pereira et al., 2009).

EC_{50} is the concentration required to achieve a 50% of radical scavenging activity. It is a commonly applied parameter to determine the antioxidant capacity and compare the antioxidant activity with different compounds. The lower EC_{50} value indicates the stronger the antioxidant activity; whereas the higher EC_{50} value shows weaker activity. In this study, the EC_{50} of the aqueous extract and different ratios of silver nanoparticles are comparable to that of ascorbic acid. The presence of antioxidant in both the aqueous extract and silver nanoparticles contributes to the significant antioxidant activity (Chen et al., 2012).

Ascorbic acid is a free radical scavenger which is water soluble. It can regenerate vitamin E in the cell membranes together with glutathione. Ascorbic acid turns into ascorbate radical when it donates an electron to the lipid radical to stop the chain reaction of lipid peroxidation. The ascorbate radicals interact rapidly to generate ascorbate and dehydroascorbate. Dehydroascorbate have no antioxidant activity. Thus, dehydroascorbate will convert back to ascorbate through the addition of two electrons. The addiction of electrons has been postulated to be performed by oxidoreductase. Due to this mode of action, ascorbic acid is

potential radical scavenger that traps detrimental free radicals and thus showed higher radical scavenging activity in this study (Nimse and Pal, 2015).

5.4 MTT Assay

In the present study, HeLa cells were incubated for 24 hours with different concentrations of samples. The highest cytotoxic activity was shown by aqueous extract with IC_{50} value of 2.144 µg/mL. As for the HT-29 cells, the highest cytotoxic activity was found in AgNPs at ratio 1:1 with IC_{50} value of 2.747 µg/mL after 48 hours incubation only. The strong cytotoxicity of both aqueous extract and silver nanoparticles towards cancer cell lines might due to the presence of phytochemicals that work in a synergistic manner to enhance the cytotoxic effect. The interactions between the phytochemical constituents may substantially affect the overall biological activities (Ristić et al., 2016).

For HeLa cells, the lowest cytotoxic activity was observed in AgNPs at ratio 9:1 with IC_{50} value of 2.145 µg/mL. On the other hand, for HT-29 cells, aqueous extract has the lowest cytotoxic activity with the IC_{50} of 2.836 µg/mL after 24 hours incubation. The lower cytotoxic effect could be attributable to the antagonistic interaction of the phytochemicals that are coated on the surface of silver nanoparticles. Due to the complex structure of the phytochemicals, the phytochemical can act differently, either synergistically or antagonistically (Zengin et al., 2014).

The signal generated from MTT assay used in this study highly dependent on the MTT concentration, the number of viable cells, metabolic activity of the cells and the duration of incubation. Of all the parameters, duration of incubation was investigated in HT-29 cells. HT-29 cells were incubated at 24 and 48 hours. With longer incubation time, the accumulation of color will occur and thus enhance the sensitivity of the MTT assay on the HT-29 cells (Riss et al., 2013). HT-29 cells was incubated for longer time period due to the silver nanoparticles may take time to diffuse into the cells to exert cytotoxic effect. The uptake of silver nanoparticles require times as they enter the cells via many pathways such as diffusion, phagocytosis and endocytosis (Sutradhar and Amin, 2014).

IC_{50} refers to the concentration of drug which reduces the cell viability by 50% (Kar et al., 2014) and were interpolated from dose response curve. For HeLa cells, a slight differences was observed between aqueous extract and different ratios of AgNPs as compared to doxorubicin hydrochloride. Both aqueous extract and AgNPs at ratio 1:9 demonstrated lowest IC_{50} of 2.144 µg/mL, respectively at 24 hours incubation. Whereas for HT-29 cells, the lowest IC_{50} was recorded for AgNPs at ratio 1:1 of 2.747 µg/mL after 48 hours incubation. According to the guidelines from the American National Cancer Institute (NCI), a crude extract with the IC_{50} of less than 20 µg/mL is recognized as highly cytotoxic. The result of the present study showed that the treatments were highly cytotoxic against HeLa and HT-29 cells due to the IC_{50} values that fall within the NCI recommended criteria. Thus, it can be predicted that aqueous extract and AgNPs at ratio 1:1 and 1:9 exhibited promising anticancer properties (Vijayarathna and Sasidharan, 2012).

Flavonoids are found abundantly in *A.scopariae* and having excellent anticancer activity. Flavonoids can induce cancer cell apoptosis. Cell death occurs as in order to eliminate damaged or unwanted cells (Chahar et al., 2011). Dysregulated apoptosis may eventually lead to oncogenesis. Flavonoids can induce apoptosis in several cancer cell lines while do not affect the survival of healthy cells. At the molecular level, the mode of action for flavonoids to induce apoptosis is not clear. Some possible mechanisms are inhibition of DNA topoisomerase I/II, alteration of signaling pathways, reducing level of nuclear transcription factor kappa B, heat shock protein expression, inhibition of Mcl-1 protein and endonuclease activation. Flavonoids causes cell cycle arrest by perturbation of checkpoints of G1/S and G2/M of the cell cycle and inhibiting all cyclin dependent kinases (CDKs). CDKs is one of the key regulators of in cell cycle progression and with the suppression of CDKs activity, thus the cell cycle will be arrested (Chahar et al., 2011).

Doxorubicin hydrochloride is classified as anthracycline drug which was derived from *Streptomyces peucetius var. caesius* and commonly used in cancers therapy targeting breast, thyroid, lung and ovarian cancers. Doxorubicin cause cytotoxicity in cancer cells by intercalating into DNA, disrupting the topoisomerase-II-mediated repair and also the production of free radicals which cause damages to DNA and proteins (Thorn et al., 2011). Based on the results, HT-29 cells were resistant to doxorubicin hydrochloride as the IC_{50} increases slightly at longer incubation Multidrug-resistant protein recognizes doxorubicin as one of the substrate and thus cause the inactivation of doxorubicin. For instance, P-glycoprotein, a membrane protein of tumor cells serve as ATP-

dependent flux pump reduces the concentrations of doxorubicin in the cancer cells (Melguizo et al., 2015).

5.5 Limitation of Study

The limitation in this study are the insufficient characterization of the green synthesized silver nanoparticles. The silver nanoparticles were given for SEM and XRD analysis, however, the equipment are out of order at the moment. Therefore, more analysis should be performed in order to give a detailed data on the characterization of the silver nanoparticles.

The other limitations is that the study is the cancer cells HeLa and HT-29 cells were unevenly plated. Therefore, the plating was repeated for many times. It is also very time-consuming to culture cancer cells

The yield of synthesized silver nanoparticles was very less and insufficient to be used to perform many assays due to the longer time taken for lyophilization.

5.6 Future Studies

The further characterizations of silver nanoparticles are important and more related analysis of silver nanoparticles should be performed. The characterization using transmission electron microscopy (TEM), dynamic light scattering (DLS), X-ray photoelectron spectroscopy (XPS), Fourier transform

infrared spectroscopy (FTIR) and atomic force microscopy (AFM) are a few analysis to further confirmed silver nanoparticles (Zhang et al., 2016).

More cancer cell lines, preferably both anchorage-dependent and anchorage independent cell lines should be considered in the cytotoxicity of the green synthesized silver nanoparticles. Normal cell lines also can be included in the cytotoxic study in silver nanoparticles to obtain reliable and significant results.

To validate the result of antioxidant activity of silver nanoparticles, more bioassays should be carried out. The antioxidant assays such as trolox equivalent antioxidant capacity (TEAC), ABTS radical scavenging assay, ferric reducing antioxidant power (FRAP), determination of total phenolic and total flavonoid content are some assays to be considered (Rajurkar and Hande, 2011). Furthermore, more cytotoxic assays such as ATP assay of cell viability, Resazurin reduction cell viability assay and LDH-release cytotoxicity assay can be performed to examine the cytotoxicity of silver nanoparticles (Riss et al., 2003). Apart from that, *in vivo* study using animal model should be carried out instead of conducting *in vitro* study alone.

CHAPTER 6

CONCLUSIONS

Aqueous extract of *Artemisiae scopariae* was used to synthesize different ratios of silver nanoparticles. Among these, AgNPs at ratio 9:1 showed the highest yield of 2.39%, whereas AgNPs at ratio 1:9 had the least yield of 0.03% due to the higher amount of secondary metabolites.After 24 hours synthesis, color changes were noted for all the different ratios of silver nanoparticles to reddish brown. The absorption SPR peaks of AgNPs at ratio 1:1, 1:9 and 9:1 were observed at 400, 325 and 455 nm, respectively.

In DPPH assay, aqueous extract and AgNPs at ratio 9:1 showed promising antioxidant activity with the EC_{50} of 0.013 mg/mL, respectively. In MTT assay, aqueous extract and AgNPs at ratio 1:9 exhibited cytotoxicity against HeLa cells the IC_{50} of 2.144 µg/mL, respectively after 24 hours treatment. Meanwhile, AgNPs at ratio 1:1 with the IC_{50} of 2.747 µg/mL after 48 hours treatment for HT-29 cells.

In a nutshell, the green synthesized silver nanoparticles from *Artemisiae scopariae* are potential as an antioxidant and cytotoxic agents. Further analysis are needed to confirm the presence of silver nanoparticles.

REFERENCES

Abascal, K., Ganora, L. and Yarnell, E., 2005. The effect of freeze-drying and its implications for botanical medical: a review. *Phytotherapy Research*, 19(8), pp. 655-660.

Adams, M.C.B., Benzon, H.T. and Hurley, R.B., 2014. 58-chemical neurolytic blocks. In: *Practical management of pain*. 5th ed. Elsevier, pp. 784-793.

Ahmed, S., Mudasir, A., Swami, B.L. and Ikram, S., 2016. A review on plants extract mediated synthesis of silver nanoparticles for antimicrobial applications: A green expertise. *Journal of Advanced Research*, 7(1), pp. 17-28.

Amin, M., Anwar, F., Janjua, M.R.S.A., Iqbal, M.A. and Rashid, U., 2012. Green synthesis of silver nanoparticles through reduction with *Solanum xanthocarpum* L. berry extract: characterization, antimicrobial and urease inhibitory activities against *Helicobacter pylori*. *International Journal of Molecular Sciences*, 13(8), pp. 9923-9941.

Aziz, S.B., Abdullah, O.G., Saber, D.R., Rasheed, M.A. and Ahmed, H.M., 2017. Investigation of metallic silver nanoparticles through UV-Vis and optical micrograph techniques. *International Journal of Electrochemical Science*, 12, pp. 363-373.

Bahuguna, A., Khan, I., Bajpai, V. K. and Kang, S. C., 2017. MTT assay to evaluate the cytotoxic potential of a drug. *Bangladesh Journal of Pharmacology*, 12, pp. 115-118.

Carmona, E. R., Benito, N., Plaza, T. and Recio-Sánchez, G., 2017. Green synthesis of silver nanoparticles by using leaf extracts from the endemic *Buddleja globose* Hope. *Green Chemistry Letters and Reviews*, 10, pp. 250-256.

Cha, J.D. et al., 2005. Chemical composition and antimicrobial activity of the essential oils of *Artemisia scoparia* and *A. capillaris. Plant Medica*, 71(2), pp. 186-190.

Chahar, M. K., Sharma, N., Dobhal, M. P. and Joshi, Y. C., 2011. Flavonoids: a versatile source of anticancer drugs. *Pharmacognosy Review*, 5(9), pp. 1-12.

Chen, Z., Bertin, R. and Froldi, G., 2012. EC_{50} estimation of antioxidant activity in DPPH assay using several statistical programs. *Food Chemistry*, 138(1), pp. 414-420.

Choi, E., Park, H., Lee, J. and Kim, G., 2013. Anticancer, antiobesity, and anti-inflammatory activity of *Artemisia* species *in vitro*. *Journal of Traditional Chinese Medicine*, 33(1), pp. 92-97.

Database of Medicinal and Aromatic Plants in Rajasthan, 2016, *Artemisia scoparia* [Online]. Available at: http:// bioinfo.bisr.res.in /project/domap/plant _ details.php?plantid=0065&bname=Artemisia%20scoparia [Accessed: 25 February 2019].

Gurunathan, S., Raman, J., Malek, S.N.A., John, P.A. and Vikineswary, S., 2013. Green synthesis of silver nanoparticles using *Ganoderma neo-japonicum* Imazeki: a potential cytotoxic agent against breast cancer cells. *International Journal of Nanomedicine*, 8, pp. 4399-4413.

Habib, M. and Waheed, I., 2013. Evaluation of anti-nociceptive, anti-inflammatory and antipyretic activities of *Artemisia scoparia* hydromethanolic extract. *Journal of Ethnopharmacology*, 145(1), pp. 18-24.

He, Y. et al., 2017. Green synthesis of silver nanoparticles using seed extract of *Alpinia katsumadai*, and their antioxidant, cytotoxicity, and antibacterial activities. *Royal Society of Chemistry*, 7, pp. 39842-39851.

Heydari, R. and Rashidipour, M., 2015. Green synthesis of silver nanoparticles using extract of oak fruit hull (Jaft): synthesis and *in vitro* cytotoxic effect on MCF-7 Cells. *International Journal of Breast Cancer*, pp. 1-6.

Kar, S. et al., 2014. Expression profiling of DNA methylation-mediated epigenetic gene-silencing factors in breast cancer. *Clinical Epigenetics*, 6(20), pp.1-13.

Kedara, S. B. and Singh, R. P., 2011. Genesis and development of DPPH method of antioxidant assay. *Journal of Food Science and Technology*, 48(4), pp. 412-422.

Keshari, A.K. et al., 2018. Antioxidant and antibacterial activity of silver nanoparticles synthesized by *Cestrum nocturnum*. *Journal of Ayurveda and Integrative Medicine*, pp.1-8.

Kumar, R., Ghoshal, G., Jain, A. and Goyal, M., 2017. Rapid green synthesis of silver nanoparticles using (*Prunus persica*) plants extract: exploring its antimicrobial and catalytic activities. *Journal of Nanomedicine & Nanotechnology*, 8(4), pp. 1-8.

Labconco Corporation., 2010, *A Guide to Freeze Drying for the Laboratory* [Online]. Available at: https://pim-resources.coleparmer.com/data-sheet/labconco-guide-freeze-dry-in-lab.pdf [Accessed: 15 February 2019].

Lansdown, A.B.G., 2010. A pharmacological and toxicological profile of silver as an antimicrobial agent in medical devices. *Advances in Pharmacological Sciences*, pp. 1-16.

Mahdi-Pour, B., Jothy, S.L., Latha, L.Y., Chen, Y. and Sasidharan, S., 2012. Antioxidant activity of methanol extracts of different parts of *Lantana camara*. *Asian Pacific Journal of Tropical Biomedicine*, 2(12), pp. 960-965.

Marxen, K. et al., 2007. Determination of DPPH radical oxidation caused by methanolic extracts of some microalgal species by linear regression analysis of spectrophotometric measurements. *Sensors*, 7(10), pp. 2080-2095.

Melguizo, C. et al., 2015. Enhanced antitumoral activity of doxorubicin against lung cancer cells using biodegradable poly(butylcyanoacrylate) nanoparticles. *Drug Design, Development and Therapy*, 9, pp. 6433-6444.

Moosa, A., Allawi, M.H. and Al-Kaser, M., 2015. Process parameter for green synthesis of silver nanoparticles using leaves extract of *Aloe vera* plant. *International Journal of Multidisciplinary and Current Research*, 3, pp. 966-975.

Nambikkairaj, R.B. and Thanighaiarassu, R.R., 2018. Green fabrication of silver nanoparticles and characterization with plant leaf essential oil compound Geraniol and their antifungal activity against human pathogenic fungi. *The Pharma Innovation Journal*, 7(11), pp. 448-453.

National Cancer Institute, 2015, *What is cancer?* [Online]. Available at: https://www.cancer.gov/about-cancer/understanding/what-is-cancer [Accessed: 31 March 2019].

Nijveldt, R.J. et al., 2001. Flavonoids: a review of probable mechanism of action and potential applications. *American Society for Nutrition*, 74(4), pp. 418-425.

Nimse, S.B. and Pal, D., 2015. Free radicals, natural antioxidants, and their reaction mechanisms. *Royal Society of Chemistry*, 5, pp. 27986-28006.

Otunola, G. K., Afolayan, A. J., Ajayi, E. O. and Odeyemi, S. W., 2017. Chracterization, antibacterial and antioxidant properties of synthesized from aqueous extract of *Allium sativum*, *Zingiber officinale*, and *Capsicum frutescens. Pharmacognosy Magazine*, 13(50), pp. 201-208.

Pereira, D.M., Valentão P., Pereira, J.A. and Andrade, P.B., 2009. Phenolics: from chemistry to biology. *Molecules*, 14, pp. 2203-2211.

Prabhu, S. and Poulose, E. K., 2012. Silver nanoparticles: mechanism of antimicrobial action, synthesis, medical applications, and toxicity effects. *International Nano Letters*, 2, pp. 1-10.

Rajendran, R. et al., 2015. Green synthesis, characterization, antimicrobial and cytotoxic effects of silver nanoparticles using *Origanum heracleoticum* L. leaf extract. *International Journal of Pharmacy and Pharmaceutical Sciences*, 7(4), pp. 288-293.

Rajurkar, N. S. and Hande, S. M., 2011. Estimation of phytochemical content and antioxidant activity of some selected traditional Indian medicinal plants. *Indian Journal of Pharmaceutical Sciences*, 73(2), pp. 146-151.

Ramteke, C., Chakrabarti, T., Sarangi, B. K. and Pandey, R. A., 2013. Synthesis of silver nanoparticles of leaves of *Ocimum sanctum* for enhanced antibacterial activity. *Journal of Chemistry*, pp. 1-7

Reddy, N. J., Vali, D. N., Rani, M. and Rani, S. S., 2014. Evaluation of antioxidant, antibacterial and cytotoxic effects of green synthesized silver nanoparticles by *Piper longum* fruit. *Materials Science and Engineering*, 34, pp. 115-122.

Riss, T. L. et al., 2013, *Cell viability assays* [Online]. Available at: https://www.ncbi.nlm.nih.gov/books/NBK144065/ [Accessed: 25 March 2019].

Riss, T., O'Brien, M. and Moravec, R., 2003. Choosing the right cell-based assay for your research. *Cell Notes*, 6, pp. 6-12.

Ristić, S. et al., 2016. Phytochemical study and antioxidant, antimicrobial and anticancer activities of *Melanelia subaurifera* and *Melanelia fuliginosa* lichens. *Journal of Food Science and Technology*, 53(6), pp. 2804-2816.

Roy, P., Das, B., Mohanty, A. and Mohapatra, S., 2017. Green synthesis of silver nanoparticles using *Azadirachta indica* leaf extract and its antimicrobial study. *Applied Nanoscience*, 7(8), pp.843-850.

Safaepour, M., Shahverdi, A. R., Shahverdi, H.R., Khorramizadeh, M.R. and Gohan, A. R., 2009. Green synthesis of small silver nanoparticles using geraniol and its cytotoxicity against Fibrosarcoma-Wehi 164. *Avicenna Journal of Medical Biotechnology*, 1(2), pp. 111-115.

Sahoo, S.K. and Labhaseetwar, V., 2003. Nanotech approaches to drug delivery and imaging. *Drug Discovery Today*, 8(24), pp. 1112-1120.

Sazhina, N., Plotnikov, E., Korotkova, E., Dorozhko, E. and Voronova, O., 2018. Electrochemical oxidability of antioxidants: synergism and antagonism in mixes. *Journal of Pharmacy and BioAllied Sciences*, 10(2), pp. 60-65.

Shaik, M.R. et al., 2018. Plant-extract-assisted green synthesis of silver nanoparticles using *Origanum vulgar* L. extract and their antimicrobial activities. *Sustainability*, 10 (913), pp. 1-14.

Shukla, S., 2017. Freeze drying process: a review. *International Journal of Pharmaceutical Sciences and Research*, 2(12), pp. 3061-3068.

Singh, H. P., Mittal, S., Kaur, S., Batish, D. R. and Kohli, R. K., 2009. Chemical composition and antioxidant activity of essential oil from residues of *Artemisia scoparia*. *Food Chemistry*, 114(2), pp. 642-645.

Singh, A. and Sarin, R., 2010. *Artemisia scoparia*: A new source of Artemisinin. *Bangladesh Journal of Pharmacology*, 5, pp. 17-20.

Sutradhar, K. B. and Amin, M. L., 2014. Nanotechnology in cancer drug delivery and selective targeting. *International Scholarly Research Notices*, pp.1-12.

Swanson, B.G., 2003. Tannins and polyphenols. In: *Encyclopedia of food sciences and nutrition*. 2nd ed. Washington: Elsevier, pp. 5729-5733.

Tan, X. J. et al., 2008. Simultaneous determination of 13 bioactive compounds in herba *Artemisiae scopariae* (Yin Chen) from different harvest seasons by HPLC–DAD. *Journal of Pharmaceutical and Biomedical Analysis*, 47(4-5), pp. 847-853.

Thorn, C. F. et al., 2011. Doxorubicin pathways: pharmacodynamics and adverse effects. *Pharmacogenet Genomics*, 21(7), pp. 440-446.

University of Queensland, 2017, *Using a haemocytometer* [Online]. Available at: https://di.uq.edu.au/community-and-alumni/sparq-ed/sparq-ed-services/using-haemocytometer [Accessed: 26 March 2019].

Vijayarathna, S. and Sasidhara, S., 2012. Cytotoxicity of methanol extracts of Elaeis guineensis on MCF-7 and Vero cell lines. *Asian Pacific Journal of Tropical Biomedicine*, 2(10), pp. 826-829.

Wagner, H., Bauer, R., Melchart, D., Xiao, P.G. and Staudinger, A., 2011. Herba Artemisiae Scopariae *Yinchen*. In: Wagner H., Bauer R., Melchart D., Xiao PG. and Staudinger A. (eds) *Chromatographic fingerprint analysis of herbal medicines*. Vienna: Springer.

World Health Organization, 2018, *Cancer* [Online]. Available at: https://www.who.int/news-room/fact-sheets/detail/cancer [Accessed: 25 February 2019].

Zengin G., Uysal, A., Gunes, E. and Aktumsek. A., 2014. Survey of phytochemical composition and biological effects of three extracts from a wild plant (*Cotoneaster nummularia* Fisch. et mey): a potential source for functional food ingredients and drug formulations. *PLoS ONE*, 9(11), pp. 1-13.

Zhang, X. F., Liu, Z. G., Shen, W. and Gurunathan, S., 2016. Silver nanoparticles: synthesis, characterization, properties, applications, and therapeutic approaches. *International Journal of Molecular Sciences*, 17(9), p. 1534.

APPENDIX A

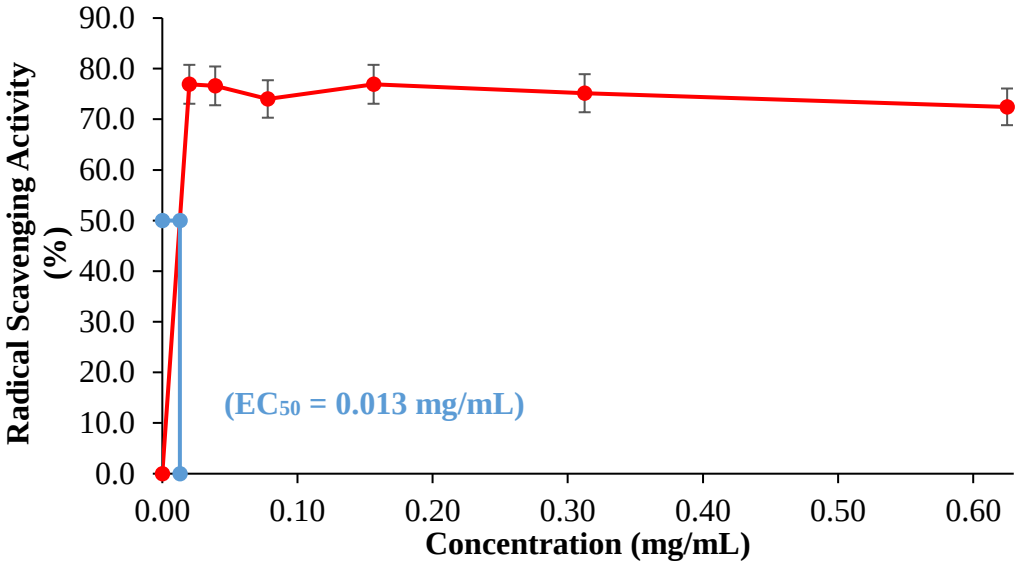

Figure A: The percentage radical scavenging activity of ascorbic acid at different concentrations.

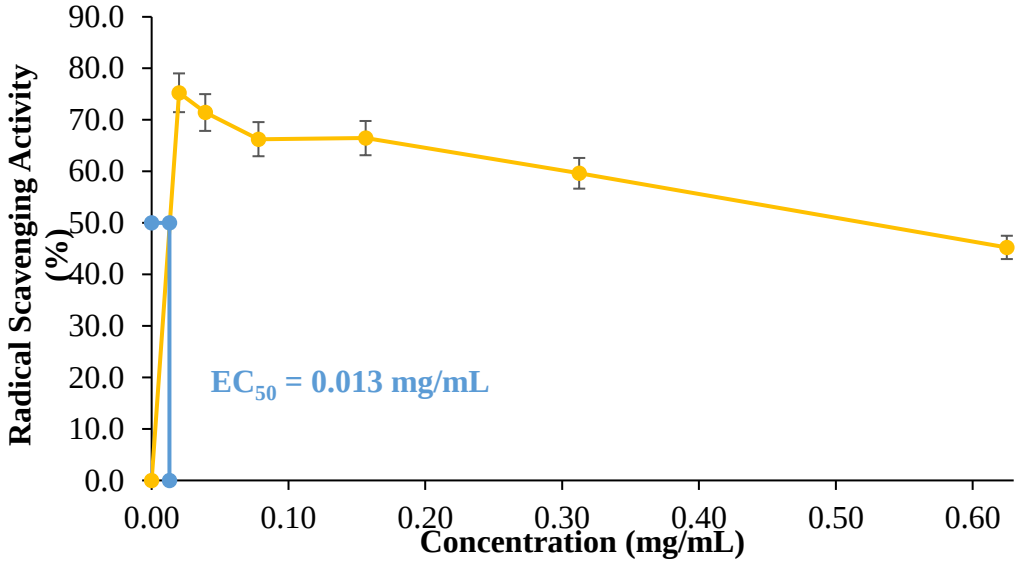

Figure B: The percentage radical scavenging activity of AgNPs at ratio 9:1 at various concentrations.

APPENDIX B

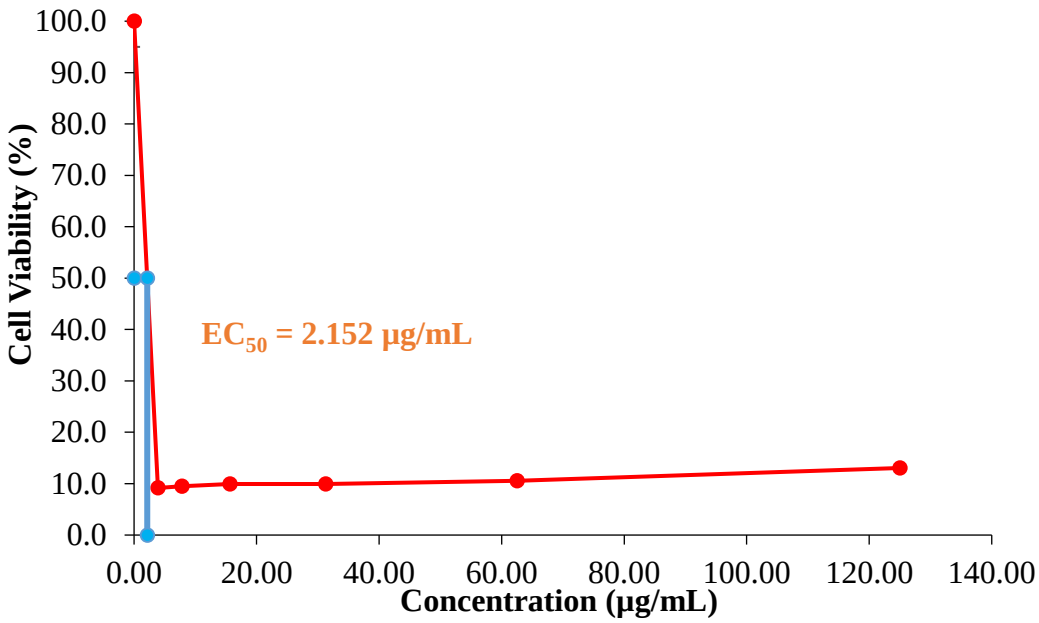

Figure C: The percentage cell viability of HeLa cells after 24 hours treated with doxorubicin hydrochloride at different concentrations.

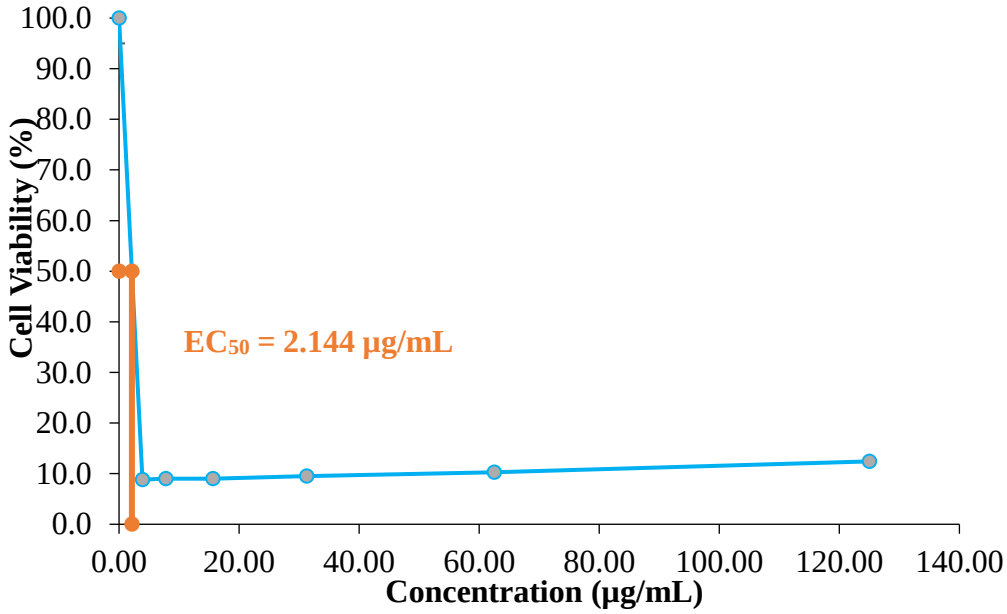

Figure D: The percentage cell viability of HeLa cells after 24 hours treatment with AgNPs at ratio 1:9 at different concentrations

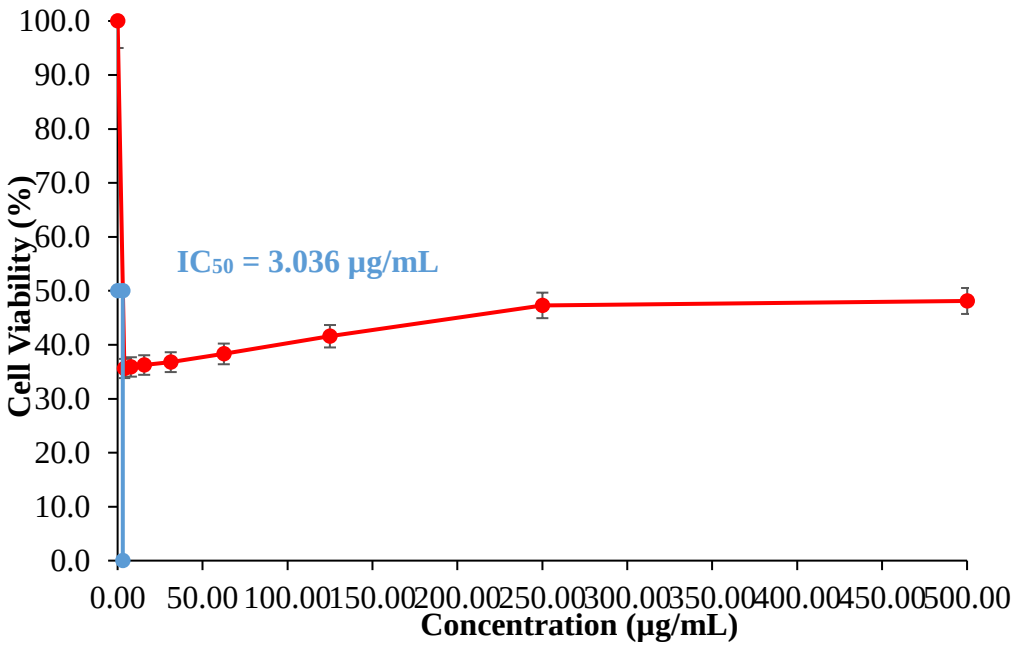

Figure E: The percentage cell viability of HT 29 cells after 48 hours treatment with doxorubicin hydrochloride at different concentrations.

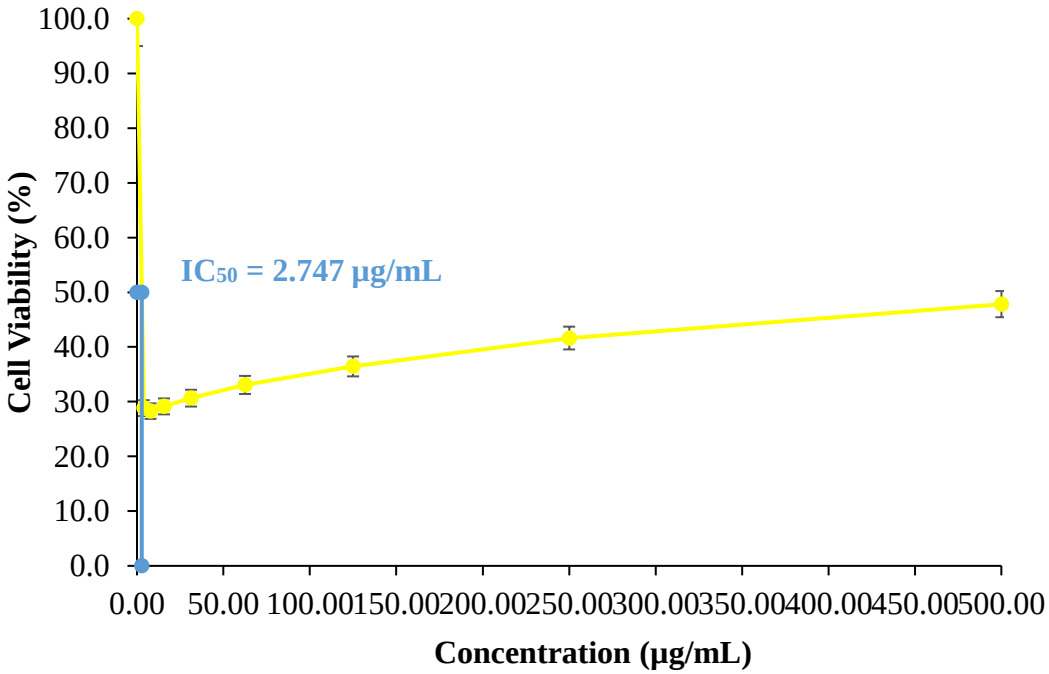

Figure F: The percentage cell viability of HT 29 cells after 48 hours treatment with AgNPs at ratio 1:1 at different concentrations.